View Article Online
View Journal

Dalton Transactions

An international journal of inorganic chemistry

Accepted Manuscript

This article can be cited before page numbers have been issued, to do this please use: G. Bottari, J. J. Moreno, V. Salazar, J. Campos, K. Mereiter, N. Rendón, J. E. Cerón-Castelán, J. Lopez-Serrano, M. Paneque and L. L. Santos, *Dalton Trans.*, 2026, DOI: 10.1039/D6DT00618C.

ROYAL SOCIETY OF CHEMISTRY

rsc.li/dalton

View Article Online
DOI: 10.1039/D6DT00618C

ARTICLE

Experimental and theoretical studies on the (co)cyclotrimerization of alkynes (and ethylene) in a TpRh compound.

Received 00th January 20xx,
Accepted 00th January 20xx

DOI: 10.1039/x0xx00000x

Giovanni Bottari,[a] Juan José Moreno,[a] Verónica Salazar,[b] Jesús Campos,[a] Kurt Mereiter,[c] Nuria Rendón,[a] Jesús Emmanuel Cerón,[b] Joaquín López-Serrano,*[a] Margarita Paneque,*[a] and Laura L. Santos,*[a]

The reactions between the Rh(I) ethylene complex $TpRh(C_2H_4)_2$ (**1**; Tp = hydrotris(pyrazolyl)borate), and the alkynes di-*tert*-butylacetylene dicarboxylate (DTBAD), acetylene, phenylacetylene, and methyl propiolate (MP) have been studied, and the results compared with those obtained previously for dimethylacetylene dicarboxylate (DMAD). Electron withdrawing groups (DTBAD) at both termini of the triple bond stabilize η^4-diene-Rh(I) species, while terminal alkynes (acetylene, phenylacetylene) easily lead to η^3-allyl-Rh(III) species. The terminal alkyne methyl propiolate, with only one electron withdrawing substituent, exhibits an intermediate behavior, forming both η^4-diene-Rh(I) and η^3-allyl-Rh(III) species. Two types of intermediate octahedral TpRh(III) rhodacycles have been detected and characterized by NMR. Mechanistic investigations by DFT are also in agreement with the intermediate role of these types of species, which form *via* oxidative coupling of compounds of type $[TpRh(C_2H_4)(C_2R_2)]$ and $[TpRh(C_2R_2)_2]$. Ligand exchange reactions to form these species from **1** are instrumental in the outcome of the reactions.

Introduction

The metal-mediated [2+2+2] cyclotrimerization of alkynes is a straightforward procedure for the synthesis of highly substituted benzene derivatives,[1] with interesting applications in organic synthesis.[2] In the presence of an olefin, a cyclohexadiene derivative may be formed instead, by the coupling of two molecules of alkyne and one of the alkene.[3] Several mechanisms have been proposed for these reactions, with the common steps of the initial formation of a metallacyclopentadiene[4] by the coupling of two molecules of alkyne in the metal complex, and the evolution of the former, by different proposed routes,[5] to the final compounds (Scheme 1).

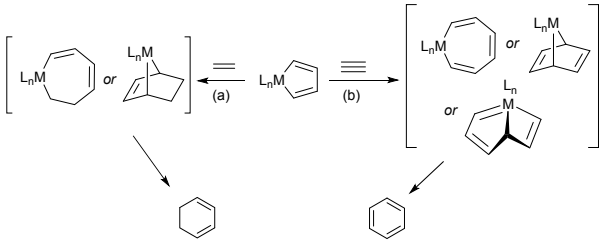

Scheme 1 Schematic, simplified representation of the evolution of a metallacyclopentadiene in the presence of (a) ethylene or (b) acetylene.

In our efforts to generate substituted benzenes via alkyne cyclotrimerization, we previously reported the reactions of two $Tp^{Me_2}Ir(I)$ complexes (Tp^{Me_2} = hydrotris(3,5-dimethylpyrazolyl)borate) with dimethyl acetylenedicarboxylate (DMAD).[6a,b] In none of these cases was the cyclotrimerization product observed, which we attributed to the reluctance of $Tp^{Me_2}Ir(III)$ species to undergo reductive elimination. In contrast, in previous studies involving the reactivity of complex $TpRh(C_2H_4)_2$ (**1**) (Tp = hydrotris(pyrazolyl)borate) toward DMAD,[6c] we observed the formation —albeit in low yield— of hexakis(methoxycarbonyl)benzene ($C_6(CO_2Me)_6$), the product of [2+2+2] cyclotrimerization of DMAD. This difference is likely due to the greater propensity of TpRh(III) intermediates to undergo reductive elimination to Rh(I) species. In fact, the reaction of complex **1** with three equivalents of DMAD resulted in a mixture of rhodium complexes along with the formation of the substituted benzene **2e** (Scheme 2). Complexes **2a**, **2b**, and **2c** are Rh(I) species featuring η^4-diene ligands, either open-chain (**2a**) or cyclic (**2b** and **2c**). In contrast, complex **2d** is an allyl Rh(III) species.

[a] *Instituto de Investigaciones Químicas, Departamento de Química Inorgánica, and Centro de Innovación en Química Avanzada (ORFEO-CINQA), Consejo Superior de Investigaciones Científicas (CSIC) and Universidad de Sevilla, Av. Américo Vespucio 49, Isla de la Cartuja, 41092 Sevilla, Spain.*
[b] *Área Académica de Químicas, Universidad Autónoma del Estado de Hidalgo, 42184 Mineral de la Reforma, Hidalgo, México.*
[c] *Department of Chemistry, Vienna University of Technology, Getreidemarkt 9/164SC, A-1060 Vienna, Austria.*

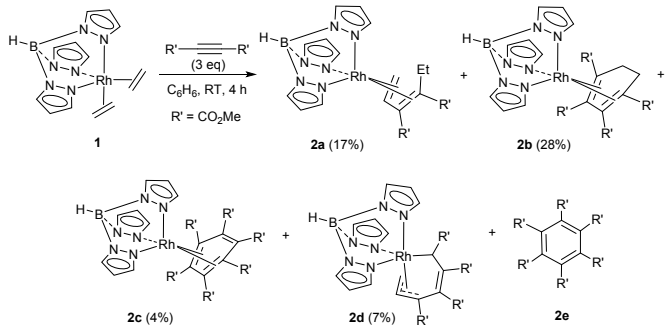

Scheme 2 Reaction of $TpRh(C_2H_4)_2$ (**1**) with 3 equivalents of DMAD (C_6H_6, 25 °C, 4 h) (isolated yields in parentheses).

We have now extended this study to a broader range of alkynes, including di-*tert*-butylacetylene dicarboxylate (DTBAD), acetylene, phenylacetylene, and methyl propiolate (MP). In addition, we have carried out a detailed mechanistic investigation of the reactions of complex **1** with acetylene and DMAD using density functional theory (DFT) calculations.

Results and discussion

Reaction of $TpRh(C_2H_4)_2$ (1) with di-*tert*butylacetylene dicarboxylate (DTBAD).

To evaluate the influence of steric effects exerted by substituents at the alkyne triple bond without altering their electronic properties, the reaction of complex **1** with 3 equivalents of di-*tert*-butylacetylene dicarboxylate (DTBAD) was carried out in benzene at room temperature. The results are summarized in Scheme 3. The major product, the Rh(I) species **3**, is analogous to compound **2a** observed in the DMAD system.[6c] Two minor species, **4** and **5**, also share the same cyclohexadiene core as **2b**, formally resulting from the coupling of two alkyne units and one ethylene fragment. However, the substituents on the organic ring occupy different positions relative to the double bonds, indicating distinct regioisomeric outcomes. These differences are attributed to steric effects imposed by the bulky *tert*-butyl groups. Surprisingly, the cyclotrimerization product was not detected in the reaction mixture. Purification of the three compounds was achieved by column chromatography (although **4** was isolated in admixture with small amounts of **5**). The excess DTBAD was also recovered through the same method.

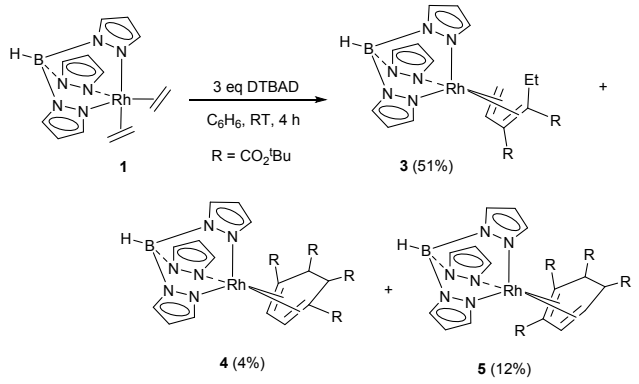

Scheme 3 Reaction of $TpRh(C_2H_4)_2$ (**1**) with DTBAD (in this and subsequent Schemes, isolated yields are shown in parentheses unless otherwise stated).

Compounds **3**, **4**, and **5** yielded single crystals upon slow evaporation of the eluent mixture (hexane/diethyl ether) and were characterized by X-ray crystallography (Figures 1 and S2 in the Supporting Information). Their solid-state molecular structures reveal several close contacts between the *tert*-butyl groups and the pyrazolyl rings of the Tp ligand, highlighting notable intramolecular steric interactions. These close contacts are forced by the steric crowding around the Rh metal center and might also play a role for the different reaction mixture compositions obtained compared to the reactions with DMAD. For instance, in compound **3** there is a CH···π interaction[7] between C(24) of a ^{t}Bu group and the pyrazolyl ring N5-N6-C7-C8-C9 of the Tp ligand. This interaction is characterized by a H···centroid distance of 2.95(4) Å and a C-H··centroid angle of 158.7(8)°. Similar parameters can be measured in the crystal structures of **4** and **5**. Other geometrical parameters, i.e. bond lengths and bond angles, are comparable to the related species discussed previously for the DMAD derivatives.[6c]

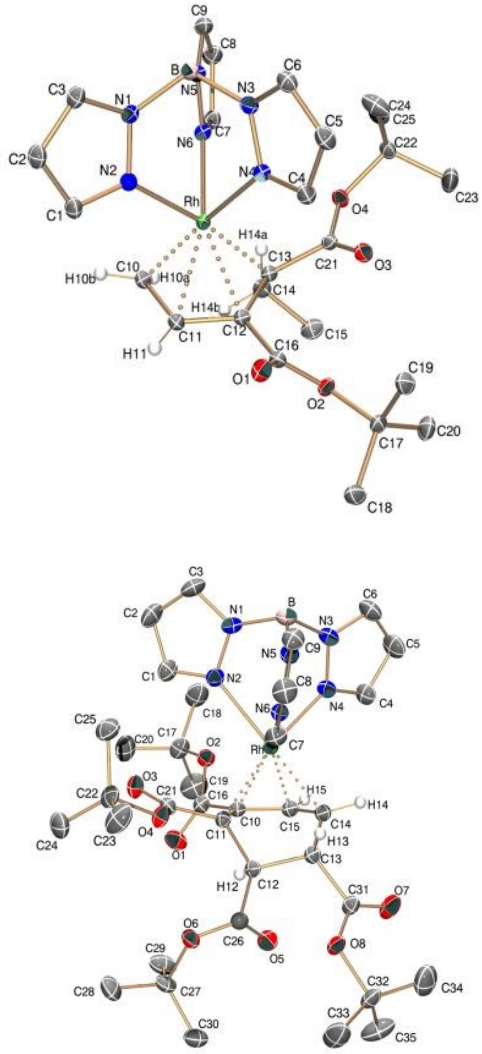

Figure 1 ORTEP diagrams of compounds **3** (up) and **5** (down). 50% thermal ellipsoids are shown. Most hydrogen atoms have been omitted for clarity. An ORTEP diagram of compound **4** is shown in Figure S2.

To gain insight into the mechanism of formation of the different rhodium species, we monitored the reaction of complex **1** with 2.5 equivalents of DTBAD in C_6D_6 at 8 °C by ^{1}H NMR spectroscopy. A new major species was observed, corresponding to the intermediate metallacyclopentene **6**,[5,8] as indicated by its characteristic NMR pattern: a resonance centered at 3.97 ppm (AA'BB' spin system, ethylene) and multiplets at 3.07, 3.02, 2.72, and 1.92 ppm, corresponding to the four inequivalent protons of the Rh–CH_2CH_2– moiety. Additionally, a second intermediate, the rhodacyclopentadiene **7**, was identified by a singlet at 4.32 ppm, attributed to the four equivalent protons of the freely rotating ethylene ligand.

Under these conditions, intermediates **6** and **7** were present in a 3:1 ratio, based on the integration of their respective ethylene ligand signals in the ^{1}H NMR spectrum. After 30 minutes at 8 °C, intermediate **7** disappeared and compound **8** was detected, while intermediate **6** underwent intramolecular transformation into the final open η^4-diene product **3**, reaching full conversion after 4 hours at room temperature. The final ratio between **3** and **8** reflects the initial 3:1 ratio between **6** and **7**, which are intermediates analogous to those previously described in the DMAD system.[6c]

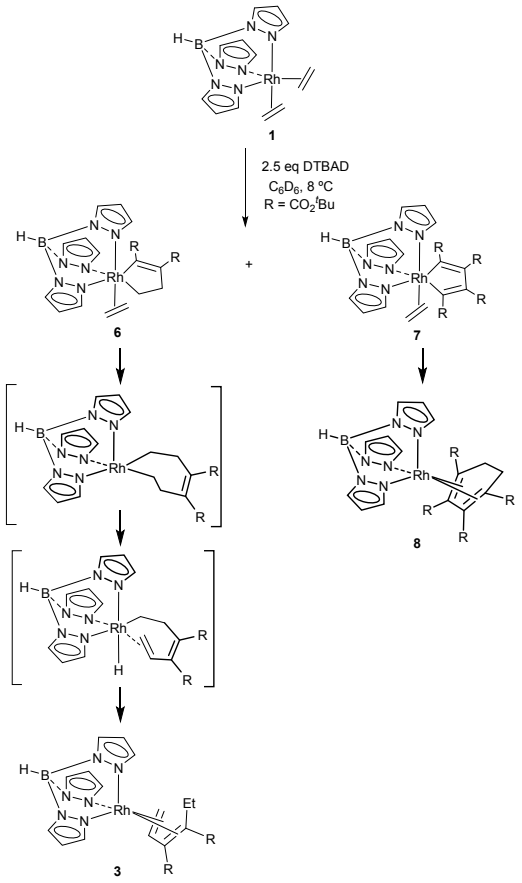

Scheme 4 Detection of intermediate species **6** and **7** by ^{1}H NMR and their evolution to **3** and **8**, respectively.

On the other hand, the mechanistic origin of compounds **4** and **5** remains uncertain due to the rearrangement observed in their carbocyclic skeletons. However, interconversion between the two isomers after formation can be ruled out, as no changes were detected upon standing the pure compounds in C_6D_6 at room temperature or upon heating at 60 °C for 24 hours. Similarly, heating compound **8** at 80 °C for 24 hours did not lead to its conversion into either of the two isomers.[9a] Nevertheless, the isomerization[9b] of this framework at a specific stage of the formation process may be favoured by the release of steric strain around the metal center, following a progression from **8** to **5** to **4** (Figure 2).

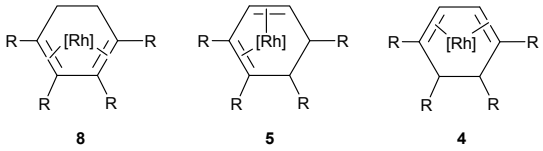

Figure 2 Schematic representation of the Rh-diene moieties of compounds **8**, **5** and **4**. [Rh] = TpRh; R = $CO_2{}^tBu$.

The molecular structure of compound **8** was postulated based on NMR analysis and subsequently confirmed by X-ray crystallography (see Supporting Information and Figure S4 for details). We propose that concentration of the alkyne plays a significant role in the formation of the intermediate metallacycles **6** and **7**, as well as in determining their relative ratio. Evidence for this effect was obtained by mixing complex **1** and 3 equivalents of DTBAD as solids in an NMR tube and heating the mixture at 50 °C for 1 hour. During this time, the alkyne acted as the solvent due to its low melting point (33–34 °C). After cooling, $CDCl_3$ was added to the tube, and the ^{1}H NMR spectrum revealed the formation of compounds **3** and **8** in an approximately 1:1 ratio. These results suggest that steric factors may hinder the exclusive formation of **8**. Notably, even in the case of the less bulky DMAD, the rhodacyclopentene intermediate of type **6** is consistently formed, regardless of the amount of alkyne used (1–8 equivalents). This observation indicates that coupling between ethylene and the alkyne is highly favourable, even in the presence of excess alkyne.

The reaction between complex **1** and DTBAD was also carried out in dichloromethane and THF. Notably, when THF was used under the same conditions described in Scheme 3 (3 equivalents of DTBAD, room temperature, 4 h), compound **8** was detected as the sole product in the crude mixture (spectrocopic yield (≥90%) and 24% isolated yield). This change in reactivity implies a role of THF medium, likely involving the replacement of the ethylene ligand in metallacycle **6**, which leads to **8** by reaction with further alkyne, as already reported in similar systems.[10]

Isolation of a stable analogue of **6** with water acting as a stabilizing agent[6a,b] is achieved when the reaction of complex **1** with 1 equivalent of DTBAD is carried out in a THF/H_2O mixture (Scheme 5). The resulting compound **9** was structurally characterized by X-ray crystallography (Figure 3). The molecular structure of **9** reveals an almost ideal octahedral geometry around the rhodium center, with minimal distortion and bond angles close to 90°. The C–C bond distances of C(12)–C(18) (1.351(2) Å) and C(10)–C(11) (1.536(2) Å) are consistent with double and single bond character, respectively. In the solid state, compound **9** forms a dimer through a characteristic hydrogen bonding motif of moderate strength, O···H–O–H···O (see Figure S6 in the Supporting Information for details).[12]

View Article Online DOI: 10.1039/D6DT01061K

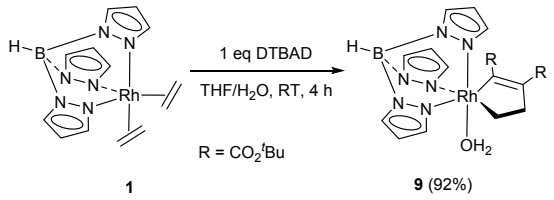

Scheme 5 Synthesis of the rhodacyclopentene **9**.

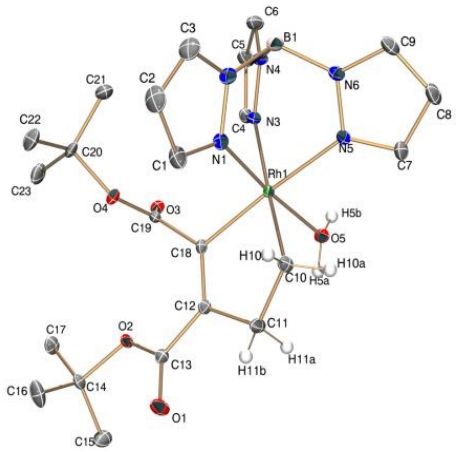

Figure 3 ORTEP diagram of compound **9**. 50% thermal ellipsoids are shown. Most hydrogen atoms have been omitted for clarity.

We have also conducted experiments aimed at obtaining the [2+2+2] cyclotrimerization product of the DTBAD monomer. In the case of DMAD, the corresponding benzene derivative is formed upon reaction of compound **2a** with an excess of alkyne, following displacement of the open-chain diene and subsequent coupling of three DMAD molecules within the TpRh coordination sphere.[6c] In contrast, heating a benzene solution of compound **3** with 6 equivalents of DTBAD at 65 °C for 12 hours resulted in no observable reaction. However, under identical conditions using 6 equivalents of DMAD, the formation of the previously reported compounds **2c** and **2e** was observed, along with dissociation of the organic diene **10** as well as compound **11**, which arises from the coupling of diene **10** with two DMAD molecules (Scheme 6). This type of transformation has already been described in the DMAD system.[6c]

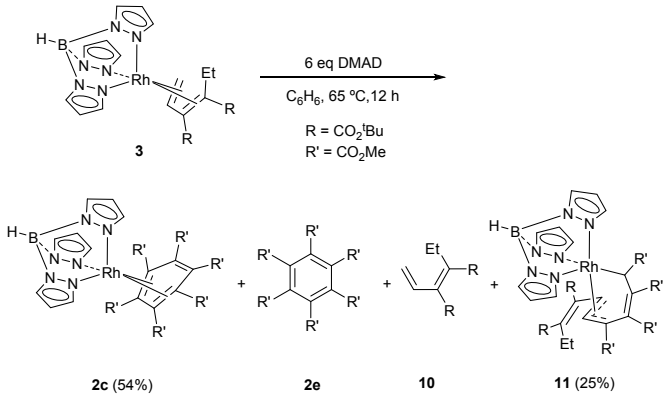

Scheme 6 Reaction of **3** with excess of DMAD (isolated yields are shown for rhodium species).

The facile generation of compound **2c** in this reaction suggests that, while **3** reacts with DMAD, DTBAD is too bulky to displace the coordinated diene and subsequently incorporate three DTBAD molecules. This steric hindrance likely prevents the formation of benzene derivatives analogous to **2c** and **2e**. Nevertheless, the detection of rhodacyclopentadiene **7** at low temperature (Scheme 4), bearing four *tert*-butyl substituents, demonstrates that such crowded intermediates are feasible. Furthermore, the [2+2+2] cyclotrimerization product of the DTBAD monomer, hexa-*tert*-butylbenzene hexacarboxylate, is a known compound and can be prepared catalytically using other metal systems.[13]

The formation of compound **11** is proposed to arise from the activation and coupling of the diene ligand in compound **3** with two additional alkyne molecules. This transformation follows a mechanism analogous to that previously postulated for the DMAD system.[6c] It involves the generation of a rhodacyclopentadiene intermediate via oxidative coupling of two DMAD molecules, along with the η^2-coordinated diene through its unsubstituted olefin moiety. Subsequent insertion of this olefin into the Rh–C bond leads to a rhodium–cycloheptadiene intermediate, which ultimately rearranges to form the (η^3-allyl)(η^1-allyl)Rh(III) complex **11**.

Reaction of $TpRh(C_2H_4)_2$ (1) with acetylene.

Treatment of **1** with acetylene (bubbling for a minute) in benzene or dichloromethane gave almost quantitative amounts of the Rh(III) compound **12** (Scheme 7). It is noteworthy that the analogous compound was only a minor species in the reaction between **1** and DMAD (**2d** in Scheme 2), and when alkyne DTBAD was employed, no allylic compound was observed (Scheme 3). Moreover, no formation of cyclic organic products such as benzene or cyclohexadiene was observed by monitoring the reaction with acetylene in CD_2Cl_2 in an NMR tube.

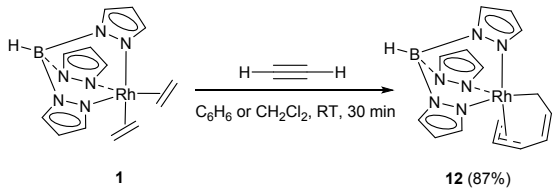

Scheme 7 Reaction of **1** with acetylene.

Furthermore, no rhodacyclopentene or rhodacyclopentadiene intermediates were detected when the reaction was carried out in C_6D_6. However, performing the reaction in acetonitrile allowed the isolation of the rhodacyclopentene **13**, as an MeCN adduct, in good yield (Scheme 8). In contrast, when a THF/H_2O mixture was used, compound **12** was observed as the major product, with no trace of the aquo-adduct. This outcome suggests a high thermodynamic stability of the allyl product **12** and its facile formation in the absence of an appropriate stabilizing agent.

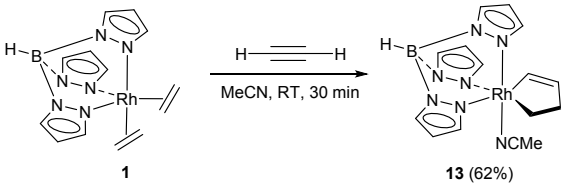

Scheme 8 Formation of the acetonitrile adduct of a rhodacyclopentene intermediate.

The reaction of complex **1** with deuterated acetylene in benzene was also carried out with the aim of confirming the structure of the product and gaining mechanistic insights into the transformation (Scheme 9).

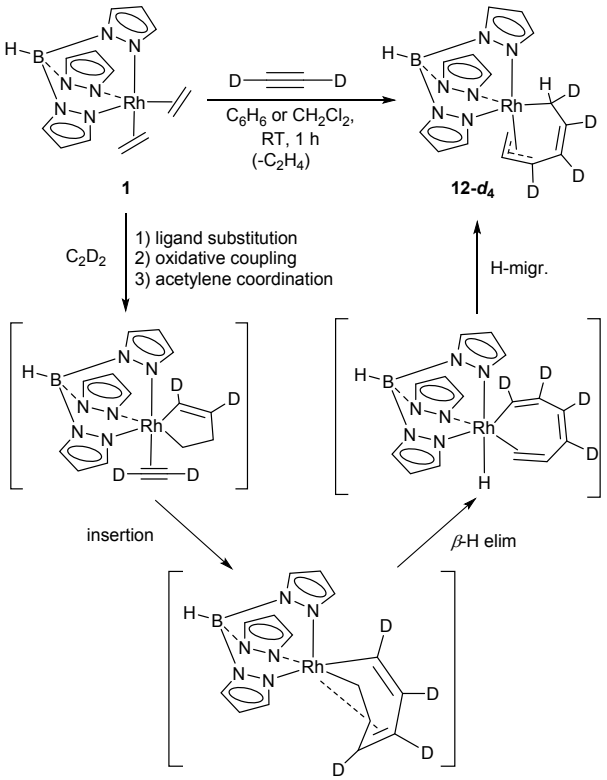

Scheme 9 Preparation of **12-*d*$_4$** by reaction of **1** with acetylene-*d*$_2$ and the pathway proposed for the transformation.

As expected, the ^{1}H NMR spectrum of compound **12-*d*$_4$** showed, aside from the resonances corresponding to the Tp ligand protons, only four signals in the 1.50–5.50 ppm region. These signals account for the CH_2–CH allylic fragment and the Rh–CDH proton, confirming the proposed structure. Scheme 9 illustrates the pathway proposed for the formation of compound **12**, based on mechanisms previously described for related Rh and Ir complexes.[6a,6c,8a,14]

Compound **12** represents a bis(allyl) complex, analogous to **11**, but with identical composition at both ends of the carbon chain (η^1-allyl and η^3-allyl). The NMR data for **12-*d*$_4$** indicates that no exchange between the two allyl termini occurs on the NMR timescale, even upon heating the sample to 80 °C for 2 hours.

We also investigated the reaction of complex **1** with acetylene in the presence of excess ethylene. The outcome of the reaction was found to depend on the relative concentrations of the two gases. Optimal results were obtained when ethylene was bubbled through the solution of compound **1** for 2.5 minutes at –60 °C, followed by a brief bubbling of acetylene for another 2.5 minutes, without interrupting the ethylene flow. Under these conditions, a new compound, **14**, was obtained as the major product (>90%) along with a variable amount of compound **12** (Scheme 10). As the amount of acetylene increased, compound **12** became the predominant species, and in some cases, the only product detected in the reaction mixture.

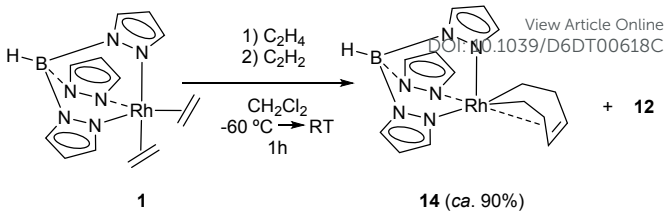

Scheme 10 Reaction of **1** with acetylene in the presence of ethylene. Spectroscopic yield of **14** shown in parentheses.

Compound **14** was isolated by column chromatography using pentane as the eluent; however, it could not be obtained in a completely pure form. Nevertheless, it was fully characterized by spectroscopic and analytical methods.

In the $^{13}C\{^1H\}$ NMR spectrum, the Rh–CH_2 moieties appear as a doublet at δ –17.4 ppm ($^1J_{CRh}$ = 16 Hz). Coordination of the double bond to the rhodium center is evidenced by the chemical shifts of the corresponding CH units: 3.94 ppm in the ^{1}H NMR and 69.7 ppm in the $^{13}C\{^1H\}$ NMR spectrum, values consistent with coordinated olefins.

An iridacyclohexene analogous to compound **14**, bearing $CO_2{}^t$Bu substituents on the olefin moiety, was previously proposed as intermediate in the formation of the iridium version of diene **3** (Scheme 4). To investigate whether a similar diene product could be obtained in this case, a solution of compound **14** in C_6D_6 was heated at 60 °C and monitored by NMR. After 3 hours, complex **14** was completely transformed into a new compound, **15** (Scheme 11). Prolonged heating at 60 °C for 24 hours did not result in further changes. Compound **14** also evolved into **15** at 25 °C over 72 hours, although the reaction under these milder conditions was not clean.

Indeed, the formation of compound **15** is analogous to that of **3**, and similarly involves a β-H elimination followed by hydride migration to the Rh–CH_2 terminus of the organic chain (Scheme 4). In the ^{1}H NMR spectrum of **15**, the –CH=CH_2 fragment coordinated to rhodium appears at δ 5.02 ppm (q, $^3J_{HH}$ ~ 7 Hz, CH), 2.01 ppm (dd, $^2J_{HH}$ ~ 3.2 Hz, $^3J_{HH}$ ~ 7 Hz, CH=C*H*H), and 1.39 ppm (m, CH=CH*H*). In the $^{13}C\{^1H\}$ NMR spectrum, the signals corresponding to this fragment are observed as doublets at 89.5 ppm (–CH) and 29.6 ppm (CH_2), due to coupling with rhodium. Additionally, the ^{1}H NMR spectrum shows that the CH_2 protons of the ethyl group are diastereotopic, appearing as two distinct multiplets at δ 1.45 and 1.00 ppm.

Finally, to determine whether compound **13** evolves into **14** in the presence of ethylene, the reaction was carried out in CH_2Cl_2 by bubbling ethylene for 3 minutes at –20 °C, followed by heating at 60 °C. After 5 hours, complete transformation of **13** into compound **15** was observed. Notably, when the reaction was performed at 25 °C, compound **15** was also formed, and **14** was not detected under either condition (Scheme 11).

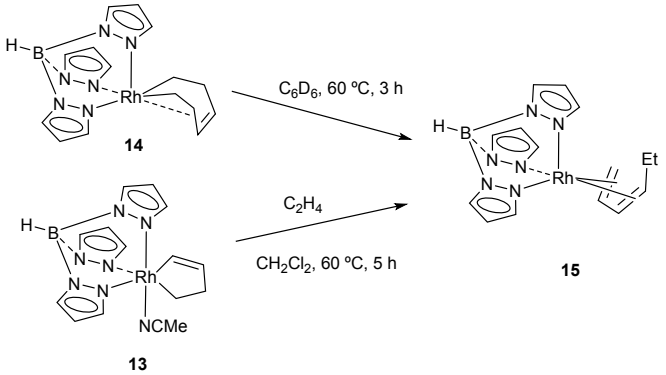

Scheme 11 Formation reaction of **15** from **13** and **14**.

Reaction of $TpRh(C_2H_4)_2$ (1) with phenylacetylene.

Additional evidence for the distinct reactivity of terminal versus internal alkynes is provided by the reaction of compound **1** with phenylacetylene, which predominantly yielded compound **16**, as depicted in Scheme 12. Minor by-products were detected in the crude mixture by ^{1}H NMR spectroscopy; however, all attempts to isolate and characterize them were unsuccessful.

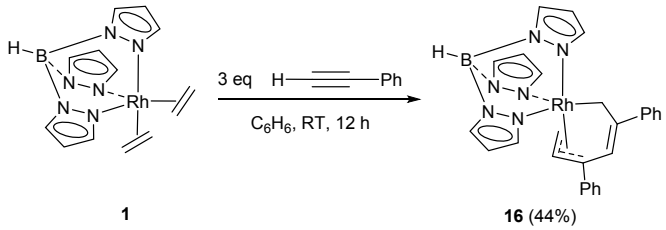

Scheme 12 Reaction of **1** with phenylacetylene.

Reaction of $TpRh(C_2H_4)_2$ (1) with methylpropiolate (MP).

Methyl propiolate (MP) exhibited an intermediate reactivity between acetylene and DMAD, predominantly affording the allyl rhodium complex **19**, along with minor amounts of compounds **17** and **18** (Scheme 13), in a manner analogous to the reaction with DMAD.

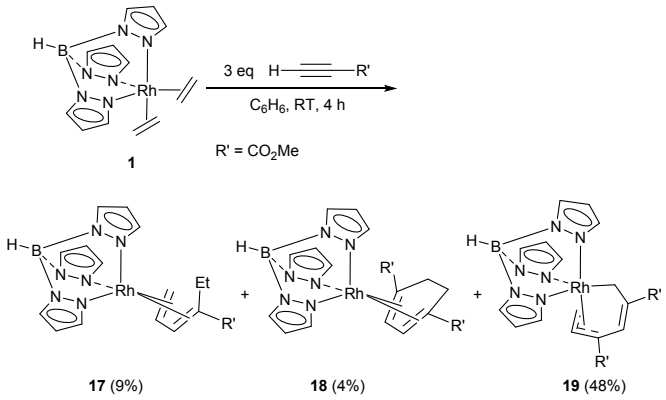

Scheme 13 Reaction of **1** with methyl propiolate.

Interestingly, the formation of compounds **16** and **19** involves the regioselective activation of phenylacetylene and MP, respectively, in such a way that the Ph and CO_2Me substituents are positioned at the β-position relative to the rhodium center. This contrasts with previously reported $Tp^{Me2}Ir$ complexes derived from MP, where alkyne insertion occurs regioselectively to place the CO_2Me group at the α-position with respect to the iridium center.[6a,15]

Computational study

Further insight into the reactivity of **1** with alkynes and ethylene was sought by Density Functional Theory methods (SMD(dichloromethane)-ωB97X-D/SDD(Rh)/cc-pVTZ// ωB97X-D /SDD(Rh)/6-31G(d,p)). This study focuses on the different outcome of reactions of **1** with acetylene and dimethylacetylenedicaboxylate (DMAD), as two relevant examples of the various alkynes used in this and previous[6c] experimental work. In the first case, the allyl Rh(III) complex **12**, is the main reaction product, whereas in the second case the electron poor alkyne DMAD promotes formation of Rh(I) complexes relevant to (co)cyclotrimerization reactions.

The mechanistic proposals discussed here are based on the experimental observations described above and elsewhere,[6c] as well as on previous mechanistic proposals on related metal systems.[5,16] Oxidative coupling in either bis-alkyne or mixed alkyne-ethylene complexes to form rhoda-cyclopentadienes or -cyclopentenes respectively is an accepted initial step in the reactivity of these systems and, as we will show in the following paragraphs, the outcome of the reactions of **1** with alkynes and ethylene will depend on the relative amount of species of type $[TpRh(C_2H_4)(C_2R_2)]$ and $[TpRh(C_2R_2)_2]$ present in the reaction mixture that can undergo oxidative coupling. Therefore, we begin by describing the formation of the former species from the bis-ethylene complex **1** (Figure 4).

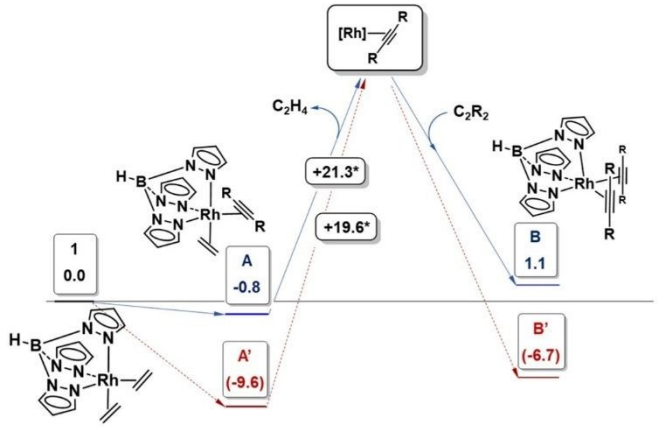

Figure 4 Stabilities of the mixed alkyne-ethylene and bis-alkyne complexes **A** and **B** (R = H, solid blue trace) and **A'** and **B'** (R = CO_2Me, dotted red trace, data in parenthesis) relative to **1** (ΔG_{qh} in dichloromethane, kcal·mol^{-1}). *Bond dissociation energies ($\Delta H°$) of ethylene in **A** and **A'** are used to approximate ligand elimination in dissociative exchange.

Ligand Exchange

Substitution of one or two ethylene ligands of **1** by acetylene to afford the mixed acetylene-ethylene species $[TpRh(C_2H_2)(C_2H_4)]$ (**A**) and the bis(alkyne) complex **B**, respectively is almost thermoneutral (ΔG_{qh} in dichloromethane = −0.8 and 1.1 kcal·mol^{-1} from **1**; see Figure 4 and the computational details). Ligand substitution can occur by either associative or dissociative pathways. In an associative mechanism coordination of acetylene, first to **1** and in a second stage to **A**, requires changing the coordination mode of their Tp ligands from κ^3 to κ^2, which is facile in both cases, with low energy barriers ($\Delta G_{qh}^{\ddagger}$) of 2.2 and 2.0 kcal·mol^{-1} from the corresponding κ^3 complexes, respectively. However, inspection by relaxed Potential Energy Surface scans of the dissociation of ethylene and acetylene from intermediates of type $[\kappa^2\text{-}TpRh(C_2H_4)_{2-n}(C_2R_2)_{1+n}]$ (n = 0, 1), containing three unsaturated ligands, indicates that the associated energy barriers are higher than those in the dissociative pathway. Thus, acetylene coordination to κ^2-**A** yields an 18-electron intermediate with two acetylenes and one ethylene, which lies 17.4 kcal·mol^{-1} above the origin (ΔG_{qh}). But, while the reverse reaction, acetylene dissociation, is almost barrier-less, dissociation of ethylene on the way to **B** adds more than 20 kcal·mol^{-1} to the overall barrier

of this route, which amounts to more than 30 kcal·mol^{-1} from **A** (Figures S7 and Figures S7a-e in the Supporting Information).

On the other hand, energy barriers for the dissociative pathway, which have been estimated as the bond dissociation energies of ethylene from the 16-electron fragments [TpRh(C_2H_4)] and [TpRh(C_2H_2)], are 22.7 and 21.3 kcal·mol^{-1}, respectively.

Alternative pathways to the formation of the alkyne and ethylene adducts of species **C** and **D** imply oxidative coupling at saturated complexes of type [κ^2-TpRh(C_2H_4)$_{2-n}$(C_2R_2)$_{1+n}$], i.e. the aforementioned intermediates in associative ligand exchange, followed by regain of the κ^3-Tp coordination. A related mechanism has been hypothesized to explain the indenyl effect and the influence

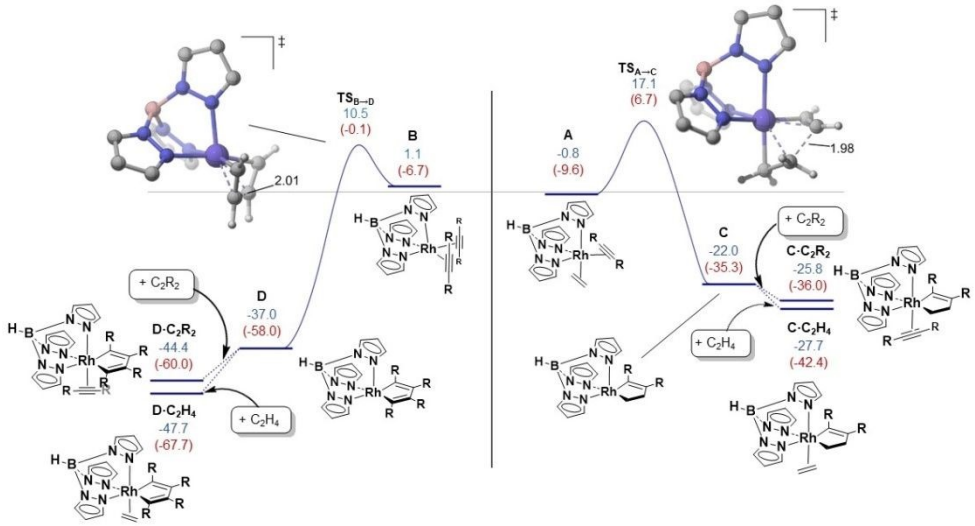

Figure 5 Gibbs Energy profile in dichloromethane (kcal·mol^{-1}) for the formation of rhodacycles **C** and **D** via oxidative coupling in the acetylene system (R = H). Data for **A'**—**D'**, with DMAD (R = CO_2Me) is given in parentheses. DFT-optimized geometries of the corresponding transition states for the acetylene system are also shown (hydrogen atoms on the Tp ligands are omitted for clarity).

Substitution of ethylene by DMAD in **1** affords **A'**, which is 9.6 kcal.mol^{-1} below the origin. It follows from this result that DMAD is a better ligand for the TpRh^{I} moiety than acetylene. Replacement of a second ethylene by DMAD offers no extra stabilization, but **B'** remains more stable than **1** by 6.7 kcal·mol^{-1}. We have not been able to locate transition states associated with ligand exchange in an associative mechanism but, analogously to the acetylene case, elimination of ethylene from the corresponding species [κ^2-TpRh(C_2H_4)$_2$(C_2R_2)], along the step sequence from **A'** to **B'** makes the overall energy barrier for this route higher than that found for the dissociative pathway, in which dissociation of ethylene from **A'** requires 19.6 kcal·mol^{-1}. Note that dissociation from **A'** is easier than from **A**, which is in line with the preference of the TpRh(I) fragment for DMAD.

Oxidative couplings. Formation of metallacycles

Oxidative coupling at **A** to give the rhodacyclopentene **C** has a barrier of 17.9 kcal·mol^{-1} and it is exergonic by 21.2 kcal·mol^{-1} (Figure 5). Transformation of **B** into the rhodacyclopentadiene **D** is both faster, $\Delta G_{qh}^{\ddagger}$ = 10.5 kcal·mol^{-1}, (overall free energy variation from **1**), and more exergonic, ΔG_{qh} = −37.0 kcal·mol^{-1}.[17] The analogous DMAD-containing species **A'** and **B'** evolve to metallacycles **C'** and **D'** through similar energy barriers than their acetylene counterparts, with oxidative coupling at the bis(alkyne) species being again faster and more favorable thermodynamically than at the mixed alkyne-ethylene complex ($\Delta G_{qh}^{\ddagger}$ = 6.6 *v.* 16.3 kcal·mol^{-1} and ΔG_{qh} = −58.0 *v.* −35.3 kcal·mol^{-1}, respectively). These results see precedent in related systems.[5g] In our case, oxidative coupling at the bis(alkyne) complexes **B** and **B'** is faster than regeneration of species **A** but, more importantly, oxidative coupling at both **A** and **B** is not reversible, with the resulting metallacycles being further stabilized by barrier-less coordination of ethylene or alkyne. While both ligands compete to form the corresponding adducts, coordination of ethylene is more favorable thermodynamically.

of the alkyne observed in the cyclotrimerization of acetylene catalysed by CpRh and Cp'Rh (Cp' = indenyl) complexes.[16a] However, in our case the barriers for oxidative coupling at these saturated intermediates exceed those found from complexes **A** and **B** (see Figure S8 in the Supporting Information).

(Co)cyclotrimerization

The following step to account for the reactivity of **1** with alkynes is C-C coupling of η^2-coordinated ethylene or alkyne to the metallacycles of **C** and **D**. Acetylene insertion into the Rh—C_{sp2} σ-bond of **C·C_2H_2** to yield **E** (Figure 6) is facile, having a barrier of 11.3 kcal·mol^{-1}, and very exergonic (ΔG_{qh} = −30.9 kcal·mol^{-1}). **E** can also be formed by ethylene insertion into one Rh—C_{sp2} σ-bond of **D·C_2H_4**, which has a barrier of 10.5 kcal·mol^{-1}, comparable to the above.[18]

Thermodynamic stability of **E** arises from coordination of the C_γ=C_δ double bond of the metallacycle with the metal to complete its 18-electron count. **E** yields **12** *via* rhodium hydride **F**, through a steps sequence that starts by isomerization of **E** through a low barrier to **E_ag**, which features a β-C—H···Rh agostic interaction. β-Elimination to afford the hydride complex **F** is almost barrier-less and takes place without change in the oxidation state of the metal. Further migration of the hydride to the Rh—C_{sp2} carbon has a barrier of 19.5 kcal·mol^{-1}. Interestingly, this step does not produce the reductive elimination product, hexatriene observed in cyclocopolymerization of ethylene and acetylene with CpCo catalysts.[5g,19] Instead, a new intermediate, **G**, forms, for which we propose a Rh(III) metallacyclopropane formulation based on a localized orbital analysis of its electronic structure (see Figures S9 in the Supporting Information).[20] Finally, **G** relaxes easily to the allyl-Rh(III) product **12**, observed experimentally. An alternative, less favorable pathway to **12** involves hydrogen migration from coordinated ethylene to one Rh—C_{sp2} carbon of the rhodacycle of **D**, followed by C-C coupling at an intermediate, **H**,

View Article Online
DOI: 10.1039/D6DT00618C

featuring alkenyl and 1-butadienyl ligands.[5g] The barrier for hydrogen transfer is 13.8 kcal·mol^{-1} from **D·C$_2$H$_4$**, compared to the 10.5 kcal·mol^{-1} found for ethylene insertion. A reason for this difference may be the Rh(V) character of the transition state for the former transformation (see Figure S10 the Supporting Information).[21] When the DMAD system is considered **E'** can be accessed either via insertion of DMAD in **C'·DMAD**, with an energy barrier of 8.8 kcal·mol^{-1}, or via ethylene insertion in **D'·C$_2$H$_4$** through a barrier of 12.1 kcal·mol^{-1}. Contrary to the acetylene system, the latter step is almost thermoneutral (ΔG_{qh} = 0.8 kcal·mol^{-1}). Regardless, the species analogous to **12** in the DMAD system, which was formed in reactions of metallacyclopentenes of type **C**·L (L = H_2O, MeCN) and DMAD,[6c] is accessible from **E'**, according to the calculations, through a mechanism parallel to that described with acetylene, albeit the overall barrier of 18.1 kcal·mol^{-1} (from **E'**) renders this transformation less favorable kinetically than in the acetylene system ($\Delta G_{qh}^{\ddagger}$ = 10.6 kcal·mol^{-1}).

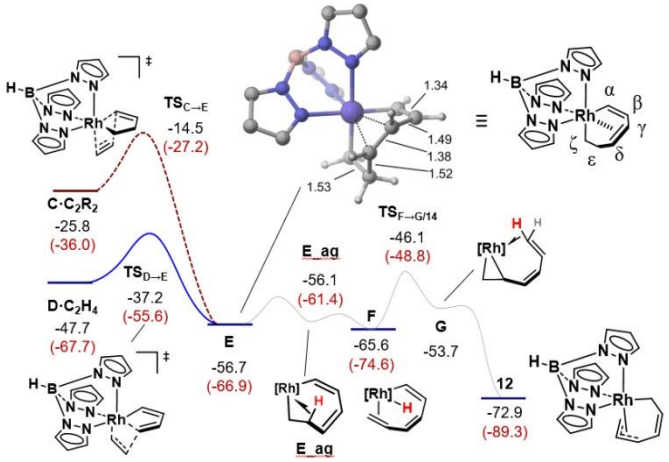

Figure 6 Gibbs Energy profile in dichloromethane (kcal·mol^{-1}) for the formation of **12**, including the structural representation of some relevant computed intermediates and transition states and the DFT-optimized geometry of **E** (with hydrogen atoms on the Tp ligands omitted for clarity). Data in parentheses are for the analogous process with the DMAD system.

To account for the competing cyclotrimerization reaction, evolution of **D·C$_2$H$_2$** was studied. Although no cyclotrimerization products have been detected with acetylene, [4+2] cycloaddition is predicted to occur at **D·C$_2$H$_2$** through a synchronous transition state that collapses directly into the Rh(I) species [TpRh(η^4-C$_6$H$_6$)] (see Scheme 2 and Figure 7).[5c,f,16b] This transformation is not reversible (ΔG_{qh} = −64.9 kcal·mol^{-1}) and the energy barrier from **D·C$_2$H$_2$** is a mere 3.8 kcal·mol^{-1}, which is significantly lower than that found for insertion of ethylene in the metallacycle of **D·C$_2$H$_4$**.

Cyclotrimerization of DMAD begins, at variance with the acetylene system, with insertion of the coordinated molecule of alkyne into one of the Rh—C$_{sp2}$ σ-bonds of **D'·DMAD** to yield the metallacycloheptatriene **J'** (Figure 7), followed by reductive coupling to afford the corresponding Rh(I) compound TpRh(η^4-C$_6$R$_6$) (R = CO_2Me). **J'** is related to intermediates proposed in the Schore mechanism for the cyclotrimerization of alkynes,[1j] but with the electron count of the metal being completed by η^2-coordination to one C=C double bond of the metallacycle, similarly to **E** and **E'**. The overall transformation is exergonic by 57.0 kcal·mol^{-1} from **D'·DMAD**, while DMAD insertion has an energy barrier of 6.9 kcal·mol^{-1}, again lower than the barrier for ethylene insertion in **D'·C$_2$H$_4$**.

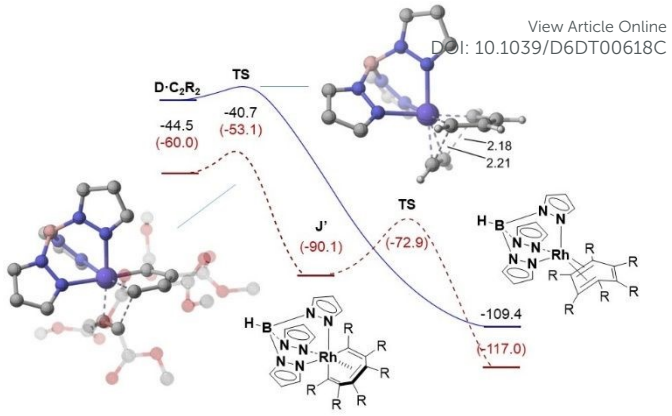

Figure 7 Gibbs Energy profiles in dichloromethane (kcal·mol^{-1}) for the final steps in the cyclotrimerization of acetylene and DMAD (dashed trace -data in parentheses-) from **D·C$_2$R$_2$** (R = H, CO_2Me) and DFT optimized geometries of the transition states for the coupling of the third alkyne (hydrogen atoms of the Tp ligands and CO_2Me groups -transparent- omitted for clarity). Energies are relative to **1** + 3 C$_2$R$_2$ – 2 C$_2$H$_4$.

To this point we have made an account of the computational results without a critical discussion of their agreement with the experiments. According to these results, both allyl-Rh(III) species and alkyne cyclotrimerization products may be accessible with acetylene and DMAD, given the relative stabilities of the calculated intermediates and energy barriers with both alkynes. However, inspection of ligand exchange kinetics and barriers for oxidative coupling reveal that formation of **B** from **A** is slower than oxidative coupling in **A** to yield **C** (the energy barriers are 21.3 kcal·mol^{-1} for ethylene dissociation from **A** compared to 17.9 kcal·mol^{-1} for oxidative coupling). According to these results, the allyl-Rh(III) species **12** may form *via* alkyne insertion at **C·C$_2$H$_2$** (Figure 6). In the DMAD system, oxidative coupling at **B'** and trapping of **D'** with DMAD lead to the Rh(I) cyclotrimerization product seen experimentally. However, the calculations predict that oxidative coupling at **A'** ($\Delta G_{qh}^{\ddagger}$ = 16.3 kcal·mol^{-1}) is also faster than ethylene dissociation (providing that formation of **B'** follows a dissociative mechanism; dissociation energy = 19.6 kcal·mol^{-1}). While we cannot offer a clear-cut explanation of the experimental observations, the calculations do show that energy barriers of the competing processes are similar enough "within the DFT error". We propose that a delicate balance exists between these barriers, which is dependent on the alkyne and on its concentration. Thus, the detection in this work of rhodacyclopentenes **9** and **13** (Schemes 5 and 8) shows formation of intermediates of type **C** that are instantly trapped by water or acetonitrile molecules that compete favorably with ethylene or acetylene. In the presence of DTBAD and DMAD,[6c] both metalla-cyclopentenes and -cyclopentadienes have been detected in their reactions with **1** as well as in reactions of the related TpIr(C$_2$H$_4$)$_2$[8a] and Tp^{Me2}Ir(C$_2$H$_4$)$_2$[6a] with DMAD. In addition, formation of the rhodacycloheptene **14** (Scheme 10) in ethylene-saturated solvent supports a role for concentration, or availability of ethylene and the alkyne in the outcome of the reaction. The calculations show that **14** can be formed as the product of the insertion of ethylene into the Rh—C_{sp2} bond of **C·C$_2$H$_4$**, which has a barrier of 14.5 kcal·mol^{-1},[18] and is exergonic by 14.7 kcal·mol^{-1}. Clearly, oxidative coupling at **A** to give **C** is preferred here to substitution of the second ethylene ligand to form **B**, which would evolve irreversibly to **D**. Then, excess ethylene traps **C**, instead of the alkyne, to form **14**.

Conclusions

The reactivity of the Rh(I) complex **1** toward a range of alkynes bearing different substituents (DTBAD, acetylene, phenylacetylene, and methyl propiolate) has been systematically investigated, and the results compared with its previously reported behaviour toward DMAD. These studies reveal that both Rh(I) and Rh(III) stable products can be selectively formed depending on the nature of the alkyne.

Alkynes bearing electron-withdrawing groups at both termini of the triple bond, such as DTBAD, preferentially stabilize η^4-diene Rh(I) species, in both open-chain and cyclic forms. In contrast, terminal alkynes (acetylene and phenylacetylene) readily evolve toward η^3-allyl Rh(III) complexes. Notably, methyl propiolate, which contains only a single electron-withdrawing substituent, exhibits intermediate reactivity, leading to the formation of both η^4-diene Rh(I) and η^3-allyl Rh(III) species.

The first step in all these reactions is the substitution of one ethylene by one alkyne and the coupling of these two unsaturated ligands (the remaining ethylene and one alkyne), to readily form rhodacyclopentenes, while in the presence of excess alkyne, substitution of both ethylenes is feasible and facile oxidative coupling yields rhodacyclopentadienes, providing access to different products.

DFT calculations support these findings and reveal that oxidative coupling is faster in bis-alkyne complexes than in mixed ethylene alkyne intermediates, in both cases the oxidative coupling is not reversible, and the resulting metallacycles further stabilized by coordination of ethylene or alkyne, being the coordination of ethylene more favorable thermodynamically. However, the oxidative coupling in mixed ethylene alkyne intermediate is faster than the formation of the bis-alkyne complex. This also agrees with the different outcome of the reactions of **1** depending on the concentration of ethylene and alkyne, highlighting the favorable coupling between ethylene and alkyne, even under conditions of alkyne excess. Both alkyne concentration and solvent nature are key factors influencing the formation of these rhodacyclic species.

Experimental Section

General methods. Manipulations were performed either in air or under oxygen-free dinitrogen atmosphere, by means of conventional Schlenk techniques. Solvents were freshly distilled prior to use over sodium/benzophenone or CaH_2 according to standard procedures. Microanalyses were conducted by the Microanalytical Service of the Instituto de Investigaciones Químicas (Sevilla). HRMS data were obtained on a JEOL JMS-SX 102A mass spectrometer by the Mass Spectrometry Services of the University of Seville (CITIUS). Infrared spectra were obtained by using Perkin–Elmer spectrometers, models 577 and 684. NMR characterization was carried out using Bruker DRX-500, DRX-400, AVANCE III-400R and DPX-300 spectrometers. Spectra were referenced to external $SiMe_4$ (δ 0 ppm) using the residual protio solvent peaks as internal standards (^1H NMR experiments) or the characteristic resonances of the solvent nuclei (^{13}C NMR experiments). Spectral assignments were performed by means of routine one- and two-dimensional NMR experiments where appropriate. $^1J(C,H)$ coupling constants were obtained from gated-^{13}C spectra. For the case of H,H coupling on a particular compound, if H_A is coupled to H_B, only the first of them appearing in the list will be accompanied by the J(AB) value. Complex $TpRh(C_2H_4)_2$,[22] **1**, was synthesized according to a procedure reported in a previous publication.[6c]

Reaction of 1 with DTBAD. To a solution of **1** (200 mg, 0.54 mmol) in benzene (15 mL), DTBAD (0.366 g, 1.62 mmol) was added as solid and the mixture was stirred for 4 h at RT. Then, the solvent was evaporated off and the residual orange solid was purified by column chromatography changing the polarity of the eluent mixture hexane/diethyl ether from 10:1 to 1:1 to yield **3** (51%), **4** (4%) and **5** (12%). Excess of DTBAD could also be recovered by chromatography.

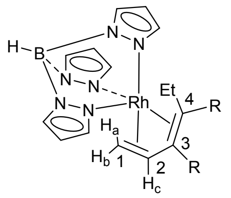

R = CO_2CMe_3

3

Compound 3. Yield: 0.165 g (51%). ^1H NMR ($CDCl_3$): δ8.02, 7.85, 7.78, 7.45, 7.25, 6.31, 6.02 (s, d, d, s, s, s, d, 1:1:1:2:1:1:2 H, $^3J_{HH}$ = 1.9 Hz, 9 CH_{ar}), 5.21 (t, $^3J_{CA,CB}$ = 7 Hz, 1 H, H_c), 2.26 (dd, $^2J_{BA}$ = 4 Hz, $^3J_{BC}$ = 7 Hz, 1 H, H_b), 2.04 (m, 1 H, H_a), 1.98, 0.97 (dq, $^2J_{HH}$ = 13 Hz, $^3J_{HH}$ = 7 Hz, 2 H, CH_2CH_3), 1.61, 0.86 (s, 9 H each, 2 CO_2CMe_3), 1.05 (t, 3 H, CH_2CH_3). $^{13}C\{^1H\}$ NMR ($CDCl_3$): δ 171.9, 168.3 (s, CO_2CMe_3), 143.9, 142.9, 139.6, 134.6, 134.2, 134.1, 105.1, 105.0, 104.3 (s, CH_{pz}), 96.7 (d, $^1J_{CRh}$ = 7 Hz, C^3), 87.4 (d, $^1J_{CH}$ = 166 Hz, $^1J_{CRh}$ = 6 Hz, C^2), 81.7, 78.3 (s, CO_2CMe_3), 43.1 (d, $^1J_{CRh}$ = 16 Hz, C^4), 31.4 (d, $^1J_{CH}$ = 160, 150 Hz, $^1J_{CRh}$ = 17 Hz, C^1), 28.1, 27.5 (s, $^1J_{CH}$ = 130 Hz, 2 CO_2CMe_3), 21.0 (s, $^1J_{CH}$ = 130 Hz, CH_2CH_3), 13.1 (s, $^1J_{CH}$ = 126 Hz, CH_2CH_3). IR (nujol): ν(C=O) 1704 cm^{-1}. Elemental analysis calcd (%) for $C_{25}H_{36}BN_6O_4Rh$: C, 50.2; H, 6.1; N, 14.1; found: C, 50.2; H, 6.0; N, 13.8.

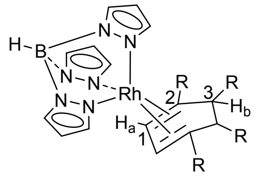

R = CO_2CMe_3

4

Compound 4. Yield: 0.016 g (4%). This compound was isolated in admixture with small amounts of compound **5**. ^1H NMR ($CDCl_3$, 25 ºC): δ 8.06, 7.78, 7.70, 7.44, 6.37, 5.94 (s, 1:1:2:2:1:2 H, 9 CH_{pz}), 6.03 (s, 2 H, 2 H_a), 3.81 (s, 2 H, 2 H_b), 1.41, 0.94 (s, 18 H each, 4 CO_2CMe_3). $^{13}C\{^1H\}$ NMR ($CDCl_3$): δ 171.5, 170.0 (s, CO_2CMe_3), 144.0, 141.7, 134.6, 134.5, 105.1, 104.7 (s, 2:1:2:1:1:2, CH_{pz}), 82.1 (d, $^1J_{CH}$ = 175 Hz, $^1J_{CRh}$ = 7 Hz, C^1), 81.2, 79.6 (s, CO_2CMe_3), 48.4 (d, $^1J_{CRh}$ = 7 Hz, C^2), 46.3 (s, $^1J_{CH}$ = 138 Hz, 5 Hz, C^3), 28.0, 27.6 (s, CO_2CMe_3). Elemental analysis calcd (%) for $C_{35}H_{50}BN_6O_8Rh$: C, 52.8; H, 6.3; N, 10.5; found: C, 53.5; H, 6.6; N, 9.5.

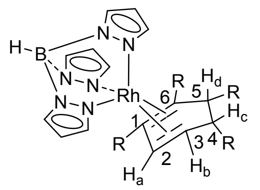

R = CO_2CMe_3

5

Compound 5. Yield: 0.051 g (12%). ^1H NMR ($CDCl_3$, 25 ºC): δ 7.92, 7.82, 7.73, 7.53, 7.45, 7.36, 6.32, 6.10, 6.00 (s, 1 H each, 9 CH_{pz}), 5.50 (d, 1 H, $^3J_{AB}$ = 5.5 Hz, H_a), 3.83 (d, 1 H, $^3J_{DC}$ = 11 Hz, H_d), 3.41 (dd, 1 H, $^3J_{BC}$ = 2.7 Hz, H_b), 3.25 (dd, H_c), 1.51, 1.47, 1.42, 1.01 (s, 9 H each, 4 CO_2CMe_3). $^{13}C\{^1H\}$ NMR ($CDCl_3$): δ 170.2, 169.3, 166.6 (s, 2:1:1, CO_2CMe_3), 143.1, 141.7, 140.8, 134.7, 134.5, 134.2, 105.4, 105.2, 104.0 (CH_{pz}), 93.2 (d, $^1J_{CRh}$ = 8 Hz, C^5), 85.4 (d, $^1J_{CH}$ = 174 Hz, $^1J_{CRh}$ = 8 Hz, C^1), 82.0, 80.9, 80.8, 79.4 (CO_2CMe_3), 46.8 (s, $^1J_{CH}$ = 130 Hz, C^3),

View Article Online
DOI: 10.1039/D6DT00618C

44.1 (d, $^1J_{CRh}$ = 15 Hz, C^6), 43.2 (s, $^1J_{CH}$ = 140 Hz, C^2), 43.2 (d, $^1J_{CH}$ = 140 Hz, $^1J_{CRh}$ = 15 Hz, C^4), 28.4, 28.1, 28.0, 27.6 (CO_2CMe_3). Elemental analysis calcd (%) for $C_{35}H_{50}BN_6O_8Rh$: C, 52.8; H, 6.3; N, 10.5; found: C, 52.2; H, 6.3; N, 9.9.

Compounds 6 and 7. To a solution of **1** (0.020 g, 0.054 mmol) in C_6D_6 (0.5 mL) in a NMR tube at 8 °C, DTBAD was added (0.012 g, 1 equiv.) and the reaction monitored by NMR to show initial formation of compound **6**. If an excess of DTBAD (0.030 g, 2.5 equiv.) was added, the ^{1}H NMR recorded upon mixture revealed instead a mixture of **6** and **7** in 2:1 ratio, before full evolution of the mixtures to the final compounds **3** and **8** (25 °C, 4 h). No elemental analysis or HRMS data could be obtained.

Selected NMR data for compound 6. ^{1}H NMR (400 MHz, C_6D_6): δ 3.97 (AA'XX' spin system, 4 H, CH_2=CH_2), 3.07, 3.02, 2.72, 1.92 (m, m, m, m, 1 H each, Rh-CH_2CH_2-). $^{13}C\{^1H\}$ NMR (101 MHz, C_6D_6): δ 170.9 (RhC_q), 135.3 ($C_q$$CH_2$), 79.5 (d, CH_2=CH_2), 36.6 (s, RhCH$_2$$CH_2$), 21.9 (d, J_{RhC} = 20 Hz, RhCH$_2$$CH_2$). **Selected NMR data for compound 7**. ^{1}H NMR (400 MHz, C_6D_6): δ 4.32 (s, 4 H, CH_2=CH_2).

Compound 8. This compound was synthesized according to the procedure described above for the reaction of **1** (0.015 g, 0.04 mmol) with DTBAD (0.027 g, 0.12 mmol) but using THF (4 h at RT) instead of benzene as the solvent. Compound **8** was purified by column chromatography on silica gel using hexane/diethyl ether (10:1) as eluent. Yield: 0.008 g (24%). Slow evaporation of a solution of the crude mixture in hexane:dichloromethane provided crystals suitable for X-ray. ^{1}H NMR (300 MHz, $CDCl_3$): δ 7.97, 7.93, 7.76, 7.44, 6.33, 5.95 (d, d, d, d, t, t, 1:2:1:2:1:2 H, $^3J_{HH}$ = 2.1 Hz, 9 CH_{pz}), 2.46, 1.01 (AA'XX' spin system, 2 H each, $^2J_{HH}$ = 10.3 Hz, 2 CH_2), 1.57, 0.92 (s, 18 H each, 4 CO_2CMe_3). $^{13}C\{^1H\}$ NMR (75 MHz, $CDCl_3$): δ 170.8, 164.8 (s, CO_2CMe_3), 144.6, 142.0, 134.2, 134.1, 104.8, 104.1 (s, 2:1:2:1:1:2, CH_{pz}), 92.9 (d, $^1J_{CRh}$ = 7 Hz, C_q-CO_2CMe_3), 82.5, 79.4 (s, CO_2CMe_3), 46.5 (d, $^1J_{CRh}$ = 15 Hz, C_q-CO_2CMe_3), 28.1, 27.4 (s, CO_2CMe_3), 23.4 (s, CH_2). Elemental analysis calcd (%) for $C_{35}H_{50}BN_6O_8Rh$: C, 52.8; H, 6.3; N, 10.5; found: C, 52.5; H, 6.1; N, 10.5. HRMS (FAB): *m/z* calcd for $C_{35}H_{50}BN_6O_8NaRh$: 819.2736; found: 819.2756 $[M + Na]^+$.

Compound 9. This compound was obtained by reaction between **1** (0.010 g, 0.03 mmol) and 1 eq of DTBAD (0.006 g, 0.03 mmol) in THF/H_2O (1 mL, 9/1) for 4 h at RT. Flash chromatography using hexane:Et_2O (1:1) yielded compound (0.009 g**,** 92%). Crystals suitable for X-ray diffraction were obtained by slow evaporation of a solution of compound **9** in chloroform. ^{1}H NMR (400 MHz, $CDCl_3$): δ 7.80, 7.66, 7.64, 7.63, 7.57, 7.31 6.19, 6.17, 6.04 (d, d, d, d, d, d, t, t, t, 1 H each, $^3J_{HH}$ = 2.3 Hz, 9 CH_{pz}), 4.26 (brs, 2 H, H_2O), 2.98, 2.88 (m, 2 H each, RhC$H_2$$CH_2$), 1.38, 0.89 (s, s, 9 H each, CO_2CMe_3). $^{13}C\{^1H\}$ NMR (101 MHz, $CDCl_3$): δ 177.9, 163.4 (CO_2CMe_3), 173.3 (d, $^1J_{CRh}$ = 31 Hz, RhC_q), 143.6, 141.6, 140.4, 135.3, 134.6, 134.4, 105.3, 105.1, 104.9 (d, s, s, s, s, s, d, s, J_{CRh} = 2 Hz, CH_{pz}), 140.4 (C_q), 79.9, 79.8 (CO_2CMe_3), 36.8 (RhCH$_2$$CH_2$), 28.4, 27.9 ($CO_2CMe_3$), 21.6 (d, $^1J_{CRh}$ = 23 Hz, RhCH$_2$$CH_2$). Elemental analysis calcd (%) for $C_{23}H_{34}BN_6O_8Rh$: C, 46.9; H, 5.8; N, 14.3; found: C, 46.9; H, 6.0; N, 14.4.

Reaction of 3 with excess of DMAD. Compound **3** (0.050 g, 0.08 mmol) was dissolved in benzene (3 mL) and excess DMAD (0.06 mL, 0.50 mmol) was added. The mixture was heated for 12 h at 65 °C, the solvent was evaporated, and the residue analyzed by ^{1}H NMR to contain a mixture of compounds **10**,[6c] **11**, **12** and **13**, which were separated by column chromatography on silica gel using hexane/diethyl ether as eluent.

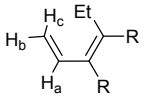

R = CO_2CMe_3

10

Compound 10. Yield: 0.009 g (38%). ^{1}H NMR (300 MHz, $CDCl_3$): δ 6.58 (dd, 1 H, $^3J_{HH}$ = 17.8, 11.1 Hz, H_a), 5.52 (d, 1 H, $^3J_{HH}$ = 17.8 Hz, H_c), 5.44 (d, 1 H, $^3J_{HH}$ = 10.9 Hz, H_b), 2.39 (q, 2 H, $^3J_{HH}$ = 7.5 Hz, C$H_2$$CH_3$), 1.54, 1.50 (s, s, 9 H each, CO_2CMe_3), 1.06 (t, 3 H, $^3J_{HH}$ = 7.5 Hz, CH_2CH_3). $^{13}C\{^1H\}$ NMR (75 MHz, $CDCl_3$): δ 167.5, 166.7 (CO_2CMe_3), 139.0 (C_q-CH_2), 135.4 (C_q-CH), 130.0 (*C*H=CH_2), 121.4 (CH=*C*H_2), 81.9, 81.3 (CO_2CMe_3), 28.2, 28.1 (CO_2CMe_3), 21.8 (CH_2CH_3), 13.4 (CH_2CH_3). HRMS (FAB): *m/z* calcd for $C_{16}H_{26}O_4Na$: 305.1729; found: 305.1725 $[M + Na]^+$.

Compound 11. Yield: 0.018 g (25%). ^{1}H NMR (400 MHz, $CDCl_3$): δ 7.91, 7.80, 7.77, 7.75, 7.53, 7.37, 6.37, 6.06, 6.02 (d, d, d, d, d, d, t, t, t, 1 H each, $^3J_{HH}$ = 2.3 Hz, 9 CH_{pz}), 7.07, 3.46 (d, d, 1 H each, $^3J_{HH}$ = 11.6 Hz, CH_{allyl}), 4.12 (d, 1 H, $^2J_{HRh}$ = 2.8 Hz, Rh-CH), 3.77, 3.76, 3.53, 2.75 (s, 3 H each, CO_2Me), 2.50 (m, 2 H, CH_2CH_3), 1.51, 0.74 (s, 9 H each, CO_2CMe_3), 1.15 (t, 3 H, $^3J_{HH}$ = 7.5 Hz, CH_2CH_3). $^{13}C\{^1H\}$ NMR (101 MHz, $CDCl_3$): δ (ppm) = 176.5, 171.6, 167.5, 167.0, 165.1, 164.7 (CO_2Me + CO_2CMe_3), 148.5 (C_q), 145.2, 144.0, 143.4, 136.1, 135.3, 134.8, 106.0, 105.3, 104.9 (CH_{pz}), 141.3 (C_q), 136.7 (C_q), 136.6 (C_q), 101.7, 67.3 (d, d, $^1J_{CRh}$ = 5, 8 Hz resp., CH_{allyl}), 81.6 (d, $^1J_{CRh}$ = 9 Hz, C_q-$_{allyl}$), 52.5, 52.4, 51.8, 50.9 (CO_2Me), 36.5, 36.3 (CO_2CMe_3), 28.3, 26.8 (CO_2CMe_3), 23.7 (CH_2CH_3), 13.2 (CH_2CH_3). Elemental analysis calcd (%) for $C_{37}H_{48}BN_6O_{12}Rh$: C, 50.3; H, 5.5; N, 9.5; found: C, 50.0; H, 5.4; N, 9.1. HRMS (FAB): *m/z* calcd for $C_{37}H_{48}BN_6O_{12}Rh$: 882.2478; found: 882.2495 $[M]^+$.

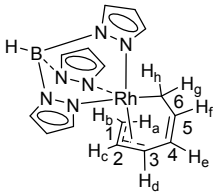

12

Compound 12. To a solution of **1** (0.100 mg, 0.27 mmol) in benzene (5 ml) in a Schlenk tube, acetylene was bubbled into the solution through a needle for approximately 1 min and the tube was sealed and left under stirring for 2 h at RT. After evaporation of solvent, compound **12** was obtained as pale-yellow solid after purification through silica gel with hexane. Yield: 93 mg (87%). ^{1}H NMR (400 MHz, $CDCl_3$): δ 7.87, 7.68, 7.62, 7.46, 6.24, 6.23, 6.13 (d, m, d, d, t, t, t, 1:3:1:1:1:1:1 H, $^3J_{HH}$ = 2.1 Hz, 9 CH_{pz}), 5.37 (m, 1 H, H_e), 5.31 (m, 1 H, H_f), 5.12 (m, 1 H, H_c), 4.97 (dt, 1 H, J_{HH} = 7.2, 2.1 Hz, H_d), 3.34 (ddt, 1 H, J_{HH} = 7.4, 1.3, 0.7 Hz, H_b), 2.57 (m, 1 H, H_g), 2.35 (dtd, 1 H, J_{HH} = 14.5, 1.9, 1.0 Hz, H_h), 1.76 (ddt, 1 H, J_{HH} = 14.5, 1.9, 1.0 Hz, H_a). $^{13}C\{^1H\}$ NMR (101 MHz, $CDCl_3$): δ 143.0, 141.3, 139.1, 135.3, 134.4, 134.1, 105.5, 105.2, 104.6 (d, d, s, s, s, s, s, s, s, $^1J_{CRh}$ = 2 Hz, CH_{pz}), 139.6 (C^5), 127.5 (C^4), 103.1 (d, $^1J_{CRh}$ = 6 Hz, C^2), 73.2 (d, $^1J_{CRh}$ = 12 Hz, C^3), 40.8 (d, $^1J_{CRh}$ = 12 Hz, C^1), 30.6 (d, $^1J_{CRh}$ = 21 Hz, C^6). Elemental analysis calcd (%) for $C_{15}H_{18}BN_6Rh$: C, 45.5; H, 4.6; N, 21.2; found: C, 46.0; H, 4.7; N, 20.8. HRMS (FAB): *m/z* calcd for $C_{15}H_{18}BN_6Rh$: 396.0741; found: 396.0746 $[M]^+$.

Compound 13. This compound was synthesized by bubbling acetylene to a solution of **1** (0.030 g, 0.08 mmol) in acetonitrile (2 mL) in a Schlenk tube for 1 minute and letting the mixture stir for 1 h at RT. Then the solvent was evaporated and the crude solid was washed with cold hexane. Yield: 0.020 g (62%). ^{1}H NMR (300 MHz, $CDCl_3$): δ 7.72, 7.69, 7.68, 7.60, 7.53, 7.45, 6.22, 6.20, 6.04 (d, d, d, d, d, d, t, t,

t, 1 H each, $^3J_{HH}$ = 2.3 Hz, 9 CH_{pz}), 6.82 (m, 1 H, RhCH), 6.24 (m, 1 H, RhCH=C*H*), 2.71, 2.55, 2.40 (m, m, s, 1:2:1 H, Rh*CH*$_2$*CH*$_2$), 2.23 (s, 3 H, MeCN). $^{13}C\{^1H\}$ NMR (75 MHz, $CDCl_3$): δ 150.4 (d, $^1J_{CRh}$ = 30 Hz, Rh*C*H), 141.0, 140.4, 140.0, 135.2, 134.7, 134.6, 105.1, 105.0 (1:1:1:1:1:1:2:1, CH_{pz}), 140.3 (RhCH=*C*H), 36.7 (Rh*C*H$_2$*C*H$_2$), 104.9 (MeCN), 22.8 (d, $^1J_{CRh}$ = 23 Hz, Rh*C*H$_2$*C*H$_2$), 4.2 (*Me*CN). Elemental analysis calcd (%) for $C_{15}H_{19}BN_7Rh$: C, 43.8; H, 4.7; N, 23.9; found: C, 43.7; H, 4.7; N, 24.0. HRMS (FAB): *m/z* calcd for $C_{15}H_{18}BN_7Rh$: 410.0766; found: 410.0760 $[M + H]^+$.

Compound 14. To a solution of **1** (0.010 g, 0.027 mmol) in CH_2Cl_2 (15 mL) in a Schlenk tube at −60 °C, ethylene was bubbled through for 2.5 minutes, after which time a tiny bubbling of acetylene was carried out for 2.5 minutes, without stopping the stream of ethylene. Then, the tube was sealed and left under stirring for 30 minutes at low temperature and then for 30 minutes at RT. After this period, the solvent was removed under reduced pressure and NMR monitoring of the crude product revealed the formation of **14** and **12** in 90:10 ratio. Compound **14** was isolated by column chromatography on silica gel using pentane as eluent although it could not be obtained in a completely pure form. ^1H NMR (400 MHz, $CDCl_3$): δ 7.91, 7.67, 7.54, 7.08, 6.25, 6.05 (s, d, d, brs, t, t, 2:2:1:1:2:1 H, $^3J_{HH}$ = 2.0 Hz, 9 CH_{pz}), 3.94 (m, 2 H, CH), 3.33, 3.26 (m, m, 2 H each, RhCH$_2$C*H*$_2$), 1.39, 0.25 (m, m, 2 H each, RhC*H*$_2$CH$_2$). $^{13}C\{^1H\}$ NMR (101 MHz, $CDCl_3$): δ 140.5, 138.3, 134.5, 134.3, 104.9, 104.7 (s, s, s, s, d, s, J_{CRh} = 3.5 Hz, CH_{pz}), 69.7 (d, $^1J_{CH}$ = 159 Hz, J_{CRh} = 5 Hz, CH), 25.9 (d, $^1J_{CH}$ = 130.2 Hz, $^1J_{CRh}$= 4 Hz, RhCH$_2$*C*H$_2$), −17.4 (d, $^1J_{CH}$ = 141 Hz, $^1J_{CRh}$ = 16 Hz, Rh*C*H$_2$CH$_2$). HRMS (FAB): *m/z* calcd for $C_{15}H_{21}BN_6Rh$: 399.0970; found: 399.0963 $[M + H]^+$.

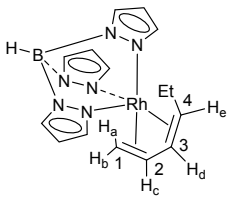

15

Compound 15. To a solution of **13** (0.040 g, 0.10 mmol) in CH_2Cl_2 (10 mL) in a Schlenk tube at −20 °C, ethylene was bubbled through a needle for 3 minutes and the tube was sealed and left under stirring for 1 h at RT and then for 5 h at 60 °C. After evaporation of solvent, compound **15** was obtained as pale-yellow solid after purification through silica gel using pentane as eluent. Yield: 0.022 g (57 %). ^1H NMR (400 MHz, C_6D_6): δ 7.93, 7.54, 7.43, 7.03, 6.02, 5.84 (brs, brs, brs, brs, brs, brs, 1:1:2:2:1:2 H, 9 CH_{ar}), 5.02 (q, $^3J_{HH}$ = 7 Hz, H_c), 4.61 (t, $^3J_{DC,DE}$ = 7 Hz, H_d), 2.55 (m, 1 H, H_e), 2.01 (dd, $^2J_{BA}$ = 3.2 Hz, $^3J_{BC}$ = 7 Hz, H_b), 1.39 (m, 1 H, H_a), 1.45, 1.00 (m, m, 1 H each, C*H*$_2$CH$_3$), 1.00 (m, 3 H, CH$_2$C*H*$_3$). $^{13}C\{^1H\}$ NMR (101 MHz, C_6D_6): δ 142.9, 139.6, 134.3, 105.2 (1:2:3:3, CH_{pz}), 89.5 (d, $^1J_{CRh}$ = 5.9 Hz, C^2), 83.8 (d, $^1J_{CRh}$ = 6 Hz, C^3), 46.0 (d, $^1J_{CRh}$ = 17.2 Hz, C^4), 29.6 (d, $^1J_{CRh}$ = 16.9 Hz, C^1), 22.1 (*C*H$_2$CH$_3$), 17.1 (CH$_2$*C*H$_3$). Elemental analysis calcd (%) for $C_{15}H_{20}BN_6Rh$: C, 45.3; H, 5.1; N, 21.1; found: C, 45.4; H, 5.3; N, 20.8. HRMS (FAB): *m/z* calcd for $C_{15}H_{21}BN_6Rh$: 399.0976; found: 399.0970 $[M + H]^+$.

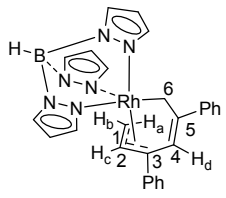

16

Compound 16 This compound was obtained by reacting compound **1** (0.030 g, 0.08 mmol) with phenylacetylene (0.025 mL, 0.24 mmol) in 3 mL of benzene. The solution was left under stirring overnight at RT, then the solvent was evaporated under vacuum and the residue purified through silica gel (pentane) to give a yellow solid. Yield: 0.019 g (44%). ^1H NMR (400 MHz, $CDCl_3$): δ 7.91, 7.70, 7.69, 7.62, 7.44, 7.14, 6.26, 6.17, 6.09 (d, 1 H each, $^3J_{HH}$ = 2 Hz, 9 CH_{pz}), 7.62 (m, 5 H, 5 CH_{ar}), 7.34, 7.29, 7.14 (m, 2:1:2, 5 CH_{ar}), 6.13 (s, 1 H, H_d), 5.83 (dd, 1 H, $^2J_{HH}$ = 11.0, 7.5 Hz, H_c), 3.39 (d, 1 H, $^3J_{HH}$ = 7.5 Hz, H_b), 3.18, 2.80 (d, 1 H each, $^3J_{HH}$ = 13.6 Hz, RhC*H*$_2$), 1.92 (d, 1 H, J_{HH} = 11.0 Hz, H_a). $^{13}C\{^1H\}$ NMR (101 MHz, $CDCl_3$): δ 147.7, 143.9 (C_{qPh}), 143.2, 140.6, 139.3, 135.3, 134.5, 134.1, 105.4, 105.2, 104.7 (CH_{pz}), 139.4 (C^5), 128.2, 128.1, 126.9, 126.0, 125.8, 125.7 (2:2:1:2:2:1, CH_{Ph}), 125.3 (C^4), 100.1 (d, $^1J_{CRh}$ = 7 Hz, C^2), 83.22 (d, $^1J_{CRh}$ = 11 Hz, C^3), 39.4 (d, $^1J_{CRh}$ = 13 Hz, C^1), 29.4 (d, $^1J_{CRh}$ = 21 Hz, C^6). Elemental analysis calcd (%) for $C_{27}H_{26}BN_6Rh$: C, 59.2; H, 4.8; N, 15.3; found: C, 59.5; H, 4.9; N, 15.0. HRMS (FAB): *m/z* calcd for $C_{27}H_{26}BN_6Rh$: 548.1367; found: 548.1387 $[M]^+$.

Reaction of 1 with methyl propiolate. To a solution of **1** (0.200 g, 0.54 mmol) in benzene (10 mL), neat MP (0.140 mL, 1.60 mmol) was added dropwise and the mixture was stirred for 4 h at RT. NMR of the crude product revealed a complex mixture of derivatives from which, after removal of volatiles, column chromatography (gradually changing the polarity of the pentane/diethyl ether eluent mixture from 8:1 to 2:1) yielded **17** (9%), **18** (4%) and **19** (48%).

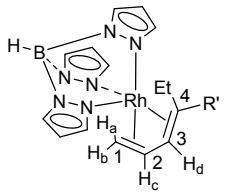

R' = CO_2Me

17

Compound 17. Yield: 0.023 g (9%). ^1H NMR (400 MHz, $CDCl_3$): δ 8.07, 7.78, 7.70, 7.56, 7.54, 7.25, 6.34, 6.06 (s, 1:1:1:1:1:1:1:2 H, 9 CH_{pz}), 6.01 (d, $^3J_{HH}$ = 5.1 Hz, H_d), 5.23 (td, $^3J_{HH}$ = 7.3, 5.1 Hz, H_c), 3.28 (s, 1 CO_2*Me*), 2.17, 1.83 (m, m, 1 H each, H_a and H_b), 2.12, 1.21 (m, m, 1 H each, C*H*$_2$CH$_3$), 0.89 (t, 3 H, $^3J_{HH}$ = 7.5 Hz, CH$_2$C*H*$_3$). $^{13}C\{^1H\}$ NMR (101 MHz, $CDCl_3$): δ 177.4 (s, *C*O$_2$Me), 142.5, 141.8, 139.7, 134.8, 134.4, 105.1, 104.3 (s, 1:1:1:1:2:2:1, CH_{pz}), 86.4 (d, $^1J_{CRh}$ = 5 Hz, C^3), 86.3 (d, $^1J_{CRh}$ = 6 Hz, C^2), 51.3 (s, CO$_2$*Me*), 47.7 (d, $^1J_{CRh}$ = 17 Hz, C^4), 31.9 (d, $^1J_{CRh}$ = 17 Hz, C^1), 22.2 (*C*H$_2$CH$_3$), 15.0 (CH$_2$*C*H$_3$). Elemental analysis calcd (%) for $C_{17}H_{22}BN_6O_2Rh$: C, 44.8; H, 4.9; N, 18.4; found: C, 44.3; H, 4.8; N, 18.9. HRMS (FAB): *m/z* calcd for $C_{17}H_{22}BN_6O_2NaRh$: 479.0850; found: 479.0851 $[M + Na]^+$.

Compound 18. Yield: 0.012 g (4%). ^1H NMR (400 MHz, $CDCl_3$): δ 8.06, 7.79, 7.68, 7.51, 6.39, 6.02 (d, d, d, d, t, t, 1:1:2:2:1:2 H, $^3J_{HH}$ = 2.3 Hz, 9 CH_{pz}), 6.16 (s, 2 H, *CH*-*CH*), 3.41 (s, 6 H, 2 CO_2Me), 2.36, 0.96 (m, m, 2 H each, C*H*$_2$C*H*$_2$). $^{13}C\{^1H\}$ NMR (101 MHz, $CDCl_3$): δ 175.1 (*C*O$_2$Me), 143.0, 142.1, 134.8, 105.5, 104.8 (2:1:3:2:1, CH_{pz}), 83.6 (d, $^1J_{CRh}$ = 7 Hz, *C*H-*C*H), 51.6 (CO$_2$*Me*), 47.7 (d, $^1J_{CRh}$ = 15 Hz, *C*CO$_2$Me), 23.1 (CH_2). Elemental analysis calcd (%) for $C_{19}H_{22}BN_6O_4Rh$: C, 44.6; H, 4.3; N, 16.4; found: C, 44.9; H, 4.5; N, 16.2. HRMS (FAB): *m/z* calcd for $C_{19}H_{22}BN_6O_4NaRh$: 535.0748; found: 535.0750 $[M + Na]^+$.

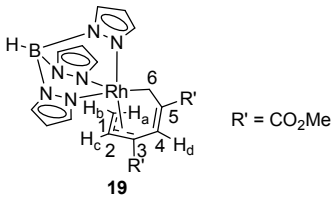

19

Compound 19. Yield: 0.132 g (48%). ^{1}H NMR (400 MHz, $CDCl_3$): δ 7.84, 7.74, 7.66, 7.61, 7.55, 6.24, 6.19, 6.13 (s, 1:1:1:1:2:1:1:1 H, 9 CH_{pz}), 6.60 (s, 1 H, H_d), 6.20 (dd, 1 H, $^3J_{HH}$ = 12.1, 7.8 Hz, H_c), 3.71, 3.53 (s, 3 H each, 2 CO_2Me), 3.60, 2.14 (d, d, 1 H each, $^3J_{HH}$ = 7.8 Hz, $^3J_{HH}$ = 12.1 Hz, H_a and H_b), 2.72, 2.63 (d, 1 H each, $^2J_{HH}$ = 14.5 Hz, RhCH$_2$). ^{13}C{^{1}H} NMR (101 MHz, $CDCl_3$): δ 172.9, 166.1 (s, *C*O_2Me), 143.7, 141.2, 140.3, 135.1, 134.8, 134.3, 105.9, 105.7, 104.6 (s, CH_{pz}), 141.8 (C^5), 137.5 (C^4), 106.7 (d, $^1J_{CRh}$ = 6 Hz, C^2), 67.9 (d, $^1J_{CRh}$ = 12 Hz, C^3), 51.9, 51.6 (s, CO_2*Me*), 47.1 (d, $^1J_{CRh}$ = 10 Hz, C^1), 27.9 (d, $^1J_{CRh}$ = 20 Hz, Rh-CH_2). Elemental analysis calcd (%) for $C_{19}H_{22}BN_6O_4Rh$: C, 44.6; H, 4.3; N, 16.4; found: C, 44.8; H, 4.2; N, 16.1. HRMS (FAB): *m/z* calcd for $C_{19}H_{22}BN_6O_4NaRh$: 535.0748; found: 535.0740 [M + Na]$^+$.

Computational details. Calculations were performed at the DFT level with the Gaussian09 program.[23] The Head-Gordon hybrid functional ωB97X-D,[24] which includes empirical dispersion, was used throughout the computational study. Geometry optimizations were carried out in the gas phase, without geometry constraints using the 6-31G(d,p) basis set[25] to represent the C, H, N and O atoms and the Stuttgart/Dresden Effective Core Potential and its associated basis set (SDD)[26] to model the Rh atoms (BS1). The stationary points of the Potential Energy Surface and their nature as minima or saddle points (TS) were characterized by vibrational analysis, which also gave gas-phase enthalpies (H), entropies (S) and Gibbs energies (G). The minima connected by a given transition state were determined by Intrinsic Reaction Coordinate (IRC) calculations or by perturbing the transition states along the TS coordinate and optimizing to the nearest minimum. The energies reported in the main text were obtained from single point calculations on the geometries previously optimized at the BS1 level using the Dunning's triple-ζ basis set cc-pVTZ[27] for C, H, N and O and also including solvent (dichloromethane) corrections with the SMD continuum model[28] (BS2). Free energy values discussed herein include corrections of the effect of the rigid-rotor harmonic oscillator treatment on thermodynamic magnitudes: ΔG_{qh}. Quasi-harmonic corrections have been carried out with the GoodVibes[29] software using the approximations of Grimme[30] for entropy and of Head-Gordon for enthalpy.[31]

Author contributions

G. B., J. E. C and V. S.: data curation, formal analysis, and investigation; J. J. M. and J. L.-S.: formal analysis (DFT); J. C. and K. M.: formal analysis (X-Ray); N. R.: investigation and writing – review & editing; J. L.-S., M. P. and L. L. S.: conceptualization, investigation, methodology, writing – review & editing.

Conflicts of interest

There are no conflicts to declare.

Data availability

View Article Online
DOI: 10.1039/D6DT00618C

The data supporting this article have been included as part of the manuscript, in the "Experimental" section, and in the Electronic Supplementary Information. See DOI: https://doi.org/10.1039/x0xx00000x

Supporting Information

The data supporting this article have been included as part of the ESI: X-ray structures for **3**, **4**, **5**, **8** and **9**, computational details and NMR spectra for compounds **3**, **4**, **5**, **8**, **9**, **10**, **11**, **13**, **14**, **15**, **16**, **17**, **18** and **19** (PDF). The supplemental file *"xyz Coordinates of calculated species"* contains the computed Cartesian coordinates of all of the molecules reported in this study. The file may be opened as a text file to read the coordinates, or opened directly by a molecular modeling program such as Mercury (version 3.3 or later, http://www.ccdc.cam.ac.uk/pages/Home.aspx) for visualization and analysis (doc).

CCDC 1411328 – 1411332 contain the supplementary crystallographic data for this paper. These data can be obtained free of charge via www.ccdc.cam.ac.uk/data_request/cif, or by emailing data_request@ccdc.cam.ac.uk, or by contacting The Cambridge Crystallographic Data Centre, 12 Union Road, Cambridge CB2 1EZ, UK; fax: +44 1223 336033.

Acknowledgements

Financial support from MCIN/AEI/10.13039/501100011033/FEDER,UE (PID2019-104159GB-100, PID2022-136570OB-I00) is gratefully acknowledged. The use of computational facilities at the Supercomputing Centre of Galicia (CESGA) and the Centro de Servicios de Informática y Redes de Comunicaciones (CSIRC, UGRGRID), Universidad de Granada (Spain) is gratefully acknowledged.

Notes and references

1 (a) Z. Li, Y. Mao, Y. Sun, B. Ma, Y. Wang, G. Zhou, Y. Zhang, F. Zeng, Z. Wang, B. Li, *Results in Chemistry*, 2024, **7**, 101523; (b) Y.-I. Wang, W.-L. Hsu, F.-C. Ho, C.-P. Li, C.-F. Wang, H.-H. Chen, *Tetrahedron*, 2017, **73**, 7210-7216; (c) K. Tanaka, *Transition-Metal-Mediated Aromatic Ring Construction*; Ed., Wiley, Hoboken, 2013; (d) D. L. J. Broere and E. Ruijter, *Synthesis*, 2012, **44**, 2639-2672; (e) S. Yamazaki, *Inorg. Chim. Acta*, 2011, **366**, 1-18; (f) G. Domínguez and J. Pérez-Castells, *Chem. Soc. Rev.*, 2011, **40**, 3430-3444; (g) B. R. Galan and T. Rovis, *Angew. Chem. Int. Ed.*, 2009, **48**, 2830-2834; (h) K. Tanaka, *Chem. Asian J.*, 2009, **4**, 508-518; (i) P. R. Chopade and J. Louie, *Adv. Synth. Catal.*, 2006, **348**, 2307-2327; (j) S. Kotha, E. Brahmachary and K. Lahiri, *Eur. J. Org. Chem.*, 2005, 4741-4767; (k) S. Saito and Y. Yamamoto, *Chem. Rev.*, 2000, **100**, 2901-2915; (l) N. E. Schore, *Chem. Rev.*, 1988, **88**, 1081-1119.

2 See for example: (a) P. Matton, S. Huvelle, M. Haddad, P. Phansavath and V. Ratovelomanana-Vidal, *Synthesis*, 2021, **54**, 4-32; (b) S. Ohta, N. Miura, K. Saitoh, K. Itoh, S. Satoh, R. Miyamoto and M. Okazaki, *Organometallics*, 2021, **40**, 2826−2835; (c) J. Miguel-Ávila, M. Tomás-Gamasa and J. L. Mascareñas, *Angew. Chem. Int. Ed.*, 2020, **59**, 17628-17633; (d) G. Wang, X. You, Y. Gan and Y. Liu, *Org. Lett.*, 2017, **19**, 110-113; (e) K. E. Ruhl and T. Rovis, *J. Am. Chem. Soc.*, 2016, **138**, 15527-15530; (f) Y. Aida, H. Sugiyama, H. Uekusa, Y. Shibata and K. Tanaka, *Org. Lett.*, 2016, **18**, 2672-2675; (g) K. Masutomi, H. Sugiyama, H. Uekusa, Y. Shibata and K. Tanaka, *Angew. Chem. Int. Ed.*, 2016, **55**, 15373-15376; (h)

F. Ye, M. Haddad, V. Michelet and V. Ratovelomanana-Vidal, *Org. Lett.*, 2016, **18**, 5612-5615; (i) H. Sato, M. Bender, W. Chen and M. J. Krische, *J. Am. Chem. Soc.*, 2016, **138**, 16244-16247; (j) M. Amatore and C. Aubert, *Eur. J. Org. Chem.*, 2015, **265**, 265-286; (k) N. Weding and M. Hapke, *Chem. Soc. Rev.*, 2011, **40**, 4525-4538.

3 (a) G. Domínguez and J. Pérez-Castells, *Chem. Eur. J.*, 2016, **22**, 6720-6739; (b) S. Alvarez, S. Medina and G. Dominguez, *J. Org. Chem.*, 2015, **80**, 2436-2442; (c) J.-P. Zhao, S.-C. Chan and C.-Y. Ho, *Tetrahedron*, 2015, **71**, 4426-4431; (d) G. Domínguez and J. Pérez-Castells in *Comprehensive Organic Synthesis II*, Second Edition, ed. P. Knochel and G. A. Molander, Elsevier, Amsterdam, 2014, pp. 1537-1581; (e) P. A. Inglesby and P. A. Evans, *Chem. Soc. Rev.*, 2010, **39**, 2791-2805; (f) J. A. Varela and C. Saá, *J. Organomet. Chem.*, 2009, **694**, 143-149 and references therein; (g) T. Shibata and K. Tsuchikama, *Org. Biomol. Chem.*, 2008, **6**, 1317-1323.

4 (a) R. S. Doerksen, T. Hodík, G. Hu, N. O. Huynh, W. G. Shuler, M. J. Krische, *Chem. Rev*. 2021, **121**, 4045-4083; (b) W. Ma, C. Yu, T. Chen, L. Xu, W.-X. Zhang and Z. Xi, *Chem. Soc. Rev.*, 2017, **46**, 1160-1192; (c) S. Kezuka, S. Tanaka, T. Ohe, Y. Nakaya and R. Takeuchi, *J. Org. Chem.*, 2006, **71**, 543-552.

5 (a) A. Roglans, A. Quintana and M. Solà, *Chem. Rev.*, 2021, **121**, 1894-1979; (b) K. Yamamoto, H. Nagae, H. Tsurugi and K. Mashima, *Dalton Trans.*, 2016, **45**, 17072-17081; (c) K. Yamamoto, H. Tsurugi and K. Mashima, *Chem. Eur. J.*, 2015, **21**, 11369-11377; (d) A. A. Dahy and N. Koga, *Organometallics*, 2015, **34**, 4965-4974; (e) L. Orian, L. P. Wolters and F. M. Bickelhaupt, *Chem. Eur. J.*, 2013, **19**, 13337-13347; (f) A. Dachs, A. Pla-Quintana, T. Parella, M. Solà and A. Roglans, *Chem. Eur. J.*, 2011, **17**, 14493-14507; (g) L. Orian, J. N. P. van Stralen and F. M. Bickelhaupt, *Organometallics*, 2007, **26**, 3816-3830; (h) V. Gandon, N. Agenet, K. P. C. Vollhardt, M. Malacria and C. Aubert, *J. Am. Chem. Soc.*, 2006, **128**, 8509-8520; (i) K. Kirchner, M. J. Calhorda, R. Schmid and L. F. Veiros, *J. Am. Chem. Soc.*, 2003, **125**, 11721-11729; (j) M. Paneque, M. L. Poveda, N. Rendón and K. Mereiter, *J. Am. Chem. Soc.*, 2004, **126**, 1610-1611; (k) W. Reppe and W. Schweckendiek, *Justus Liebigs Ann. Chem.*, 1948, **560**, 104-116.

6 (a) M. Paneque, C. M. Posadas, M. L. Poveda, N. Rendón, E. Álvarez and K. Mereiter, *Chem. Eur. J.*, 2007, **13**, 5160-5172; (b) M. Paneque, C. M. Posadas, M. L. Poveda, N. Rendón, L. L. Santos, E. Álvarez, V. Salazar, K. Mereiter and E. Oñate, *Organometallics*, 2007, **26**, 3403-3415; (c) G. Bottari, L. L. Santos, C. M. Posadas, J. Campos, K. Mereiter and M. Paneque, *Chem. Eur. J.*, 2016, **22**, 13715-13723.

7 (a) J. Pasán, J. Sanchiz, C. Ruiz-Pérez, F. Lloret and M. Julve, *Eur. J. Inorg. Chem.*, 2004, 4081-4090; (b) D. Braga, F. Grepioni and E. Tedesco, *Organometallics*, 1998, **17**, 2669-2672.

8 For examples of related 2-iridacyclopentenes see: (a) A. Vivancos, N. Rendón, M. Paneque, M. L. Poveda and E. Álvarez, *Organometallics*, 2015, **34**, 5438-5453; (b) J. M. O'Connor, A. Closson and P. Gantzel, *J. Am. Chem. Soc.*, 2002, **124**, 2434-2435.

9 (a) E. S. Johnson, G. J. Balaich and I. P. Rothwell, *J. Am. Chem. Soc.*, 1997, **119**, 7685-7693; (b) S. Biswas, Z. Huang, Y. Choliy, D. Y. Wang, M. Brookhart, K. Krogh-Jespersen and A. S. Goldman, *J. Am. Chem. Soc.*, 2012, **134**, 13276-13295.

10 A. A. Bowden, R. P. Hughes, D. C. Lindner, C. D. Incarvito, L. M. Liable-Sands and A. L. Rheingold, *J. Chem. Soc., Dalton Trans.*, 2002, 3245-3252.

11 For some examples on discussions on the participation of rhodacyclopentenes as intermediates of different reactions, see: (a) Y. Oonishi, S. Masusaki, S. Sakamoto and Y. Sato, *Angew. Chem. Int. Ed.*, 2019, **58**, 8736-8739; (b) K. Masutomi, N. Sakiyama, K. Noguchi and K. Tanaka, *Angew. Chem. Int. Ed.*, 2012, **51**, 13031-13035; (c) T. Kondo, *Synlett*, 2008, 629-644. (d) Z.-X. Yu, P. A. Wender and K. N. Houk, *J. Am. Chem. Soc.*, 2004, **126**, 9154-9155; (e) C. E. Dean, R. D. W. Kemmitt, D. R. Russell and M. D. Schilling, *J. Organomet. Chem.*, 1980, **187**, C1-C6.

12 T. Steiner, *Angew. Chem. Int. Ed.*, 2002, **41**, 48-76.

13 V. Cadierno, S. E. García-Garrido and J. Gimeno, *J. Am. Chem. Soc.*, 2006, **128**, 15094-15095.

14 (a) A. Vivancos, Y. A. Hernández, M. Paneque, M. L. Poveda, V. Salazar and E. Álvarez, *Organometallics*, 2015, **34**, 177-188; (b) M. Paneque, M. L. Poveda, N. Rendón, E. Álvarez and E. Carmona, *Eur. J. Inorg. Chem.*, 2007, 2711-2720.

15 M. Paneque, C. M. Posadas, M. L. Poveda, N. Rendón and K. Mereiter, *Organometallics*, 2007, **26**, 3120-3129.

16 (a) L. Orian, M. Swart and F. M. Bickelhaupt, *ChemPhysChem*, 2014, **15**, 219-228; (b) J. H. Hardesty, J. B. Koerner, T. A. Albright and G.-Y. Lee, *J. Am. Chem. Soc.*, 1999, **121**, 6055-6067.

17 Oxidative coupling at **1** to give a metallacyclopentane has been discarded as the energy barrier, $\Delta G_{qh}^{\ddagger}$ = 24.2 kcal·mol^{-1}, exceeds the calculated for related steps at **A** and **B**.

18 Insertion of acetylene into the Rh—Csp^3 σ-bond of **C·C$_2$H$_2$** has an energy barrier of 16.3 kcal·mol^{-1} compared to the 11.3 kcal ·mol^{-1} required for insertion into the Rh—Csp^2 bond. A similar preference is found for the insertion of ethylene at **C·C$_2$H$_4$** ($\Delta G_{qh}^{\ddagger}$ = 19.2 vs. 14.5 kcal·mol^{-1} for insertion into the Rh—Csp^3 and Rh—Csp^2 bonds respectively). This selectivity has been described for related systems, see for example ref 5h.

19 Reductive elimination from an analogous alkyl-allyl complex containing the CpCo fragment to give hexatriene has a barrier of 27.7 kcal·mol^{-1}. See ref 5g.

20 (a) J. Pipek and P. G. Mezey, *J. Chem. Phys.*, 1989, **90**, 4916-4926. For examples of application of this method to organometallic complexes see: (b) P. Vidossich and A. Lledós, *Dalton Trans.*, 2014, **43**, 11145-11151; (c) N. Curado, C. Maya, J. López-Serrano and A. Rodríguez, *Chem. Commun.*, 2014, **50**, 15718-15721.

21 J. Oxgaard, R. P. Muller, W. A. Goddard III and R. A. Periana, *J. Am. Chem. Soc.*, 2004, **126**, 352-363.

22 S. Trofimenko, *J. Am. Chem. Soc.*, 1969, **91**, 588-595.

23 Gaussian 09, Revisions B.01 and E.01, M. J. Frisch, G. W. Trucks, H. B. Schlegel, G. E. Scuseria, M. A. Robb, J. R. Cheeseman, G. Scalmani, V. Barone, G. A. Petersson, H. Nakatsuji, X. Li, M. Caricato, A. Marenich, J. Bloino, B. G. Janesko, R. Gomperts, B. Mennucci, H. P. Hratchian, J. V. Ortiz, A. F. Izmaylov, J. L. Sonnenberg, D. Williams-Young, F. Ding, F. Lipparini, F. Egidi, J. Goings, B. Peng, A. Petrone, T. Henderson, D. Ranasinghe, V. G. Zakrzewski, J. Gao, N. Rega, G. Zheng, W. Liang, M. Hada, M. Ehara, K. Toyota, R. Fukuda, J. Hasegawa, M. Ishida, T. Nakajima, Y. Honda, O. Kitao, H. Nakai, T. Vreven, K. Throssell, J. A. Montgomery Jr., J. E. Peralta, F. Ogliaro, M. Bearpark, J. J. Heyd, E. Brothers, K. N. Kudin, V. N. Staroverov, T. Keith, R. Kobayashi, J. Normand, K. Raghavachari, A. Rendell, J. C. Burant, S. S. Iyengar, J. Tomasi, M. Cossi, J. M. Millam, M. Klene, C. Adamo, R. Cammi, J. W. Ochterski, R. L. Martin, K. Morokuma, O. Farkas, J. B. Foresman and D. J. Fox, Gaussian, Inc., Wallingford CT, 2016.

24 J.-D. Chai and M. Head-Gordon, *Phys. Chem. Chem. Phys.*, 2008, **10**, 6615-6620.

25 (a) W. J. Hehre, R. Ditchfield and J. A. Pople, *J. Chem. Phys.*, 1972, **56**, 2257-2261; (b) P. C. Hariharan and J. A. Pople, *Theor. Chim. Acta.*, 1973, **28**, 213-222; (c) M. M. Francl, W. J. Pietro, W. J. Hehre, J. S. Binkley, M. S. Gordon, D. J. Defrees and J. A. Pople, *J. Chem. Phys.*, 1982, **77**, 3654-3665.

26 D. Andrae, U. Haeussermann, M. Dolg, H. Stoll and H. Preuss, *Theor. Chim. Acta*, 1990, **77**, 123-141.

27 R. A. Kendall, T. H. Dunning Jr. and R. J. Harrison, *J. Chem. Phys.*, 1992, **96**, 6796-6806.

View Article Online
DOI: 10.1039/D6DT00618C

28 A. V. Marenich, C. J. Cramer and D. G. Truhlar, *J. Phys. Chem. B*, 2009, **113**, 6378-6396.
29 G. Luchini, J. V. Alegre-Requena, Y. Guan, I. Funes-Ardoiz and R. S. Paton, GoodVibes: GoodVibes 3.0.1, 2019, http://doi.org/10.5281/zenodo.595246.
30 S. Grimme, *Chem. Eur. J.*, 2012, **18**, 9955-9964.
31 Y.-P. Li, J. Gomes, S. M. Sharada, A. T. Bell and M. Head-Gordon, *J. Phys. Chem. C.*, 2015, **119**, 1840−1850.

View Article Online
DOI: 10.1039/D6DT00618C

Data availability

The data supporting this article have been included as part of the manuscript, in the “Experimental” section, and in the Electronic Supplementary Information. See DOI: https://doi.org/10.1039/x0xx00000x